Title:

Boosting Live Malaria Vaccine with Cytomegalovirus Vector Can Prolong Immunity through Innate and Adaptive Mechanisms

Authors: Komi Gbedande[1, 2 #a], Samad A. Ibitokou[1, #b], Monique L. Ong[3, 4], Mariapia A. Degli-Esposti[3, 4], Michael G. Brown[5], Robin Stephens[1, 2, 6, *, #a]

Affiliation:

[1] Department of Internal Medicine, Division of Infectious Diseases, University of Texas Medical Branch, Galveston, TX 77555-0435

[2] Center for Immunity and Inflammation, Rutgers New Jersey Medical School, Cancer Center, 205 S. Orange Avenue, Newark, NJ 07103

[3] Centre for Experimental Immunology, Lions Eye Institute; Nedlands, Western Australia, Australia

[4] Infection and Immunity Program and Department of Microbiology, Biomedicine Discovery Institute, Monash University; Clayton, Victoria, Australia

[5] Department of Medicine, Division of Nephrology, and the Beirne B. Carter Center for Immunology Research, University of Virginia, Charlottesville, VA

[6] Department of Microbiology and Immunology, University of Texas Medical Branch, Galveston, TX

[*] **Corresponding author**

[#a] Current Address: RS, KG: Center for Immunity and Inflammation, Rutgers New Jersey Medical School, Cancer Center, 205 S. Orange Avenue, G-1230; Newark, NJ 07103;

24 [#b] Current Address SAI: Fate Therapeutics, 12278 Scripps Summit Drive, San Diego, CA 92131

25 **Short Title:** MCMV Boost Prolongs Malaria Vaccine Protection and Effector T cells

26

27 **Abstract**

28 Vaccines to persistent parasite infections have been challenging, and current iterations lack
29 long-term protection. Cytomegalovirus (CMV) chronic vaccine vectors drive protection against
30 SIV, tuberculosis and liver-stage malaria correlated with antigen-specific CD8 T cells with a Tem
31 phenotype. This phenotype is likely driven by a combination of antigen-specific and innate
32 adjuvanting effects of the vector, though these mechanisms are less well understood. Sterilizing
33 immunity from live *Plasmodium chabaudi* vaccination lasts less than 200 days. While *P.*
34 *chabaudi*-specific antibody levels remain stable after vaccination, the decay of parasite-specific T
35 cells correlates with loss of challenge protection. Therefore, we enlisted murine CMV as a booster
36 strategy to prolong T cell responses against malaria. To study induced T cell responses, we
37 included *P. chabaudi* MSP-1 epitope B5 (MCMV-B5). We found that MCMV vector alone
38 significantly protected against a challenge *P. chabaudi* infection 40-60 days later, and that
39 MCMV-B5 was able to make B5-specific Teff, in addition to previously-reported Tem, that
40 survive to the challenge timepoint. Used as a booster, MCMV-B5 prolonged protection from
41 heterologous infection beyond day 200, and increased B5 TCR Tg T cell numbers, including both
42 a highly-differentiated Tem phenotype and Teff, both previously reported to protect. B5 epitope
43 expression was responsible for maintenance of Th1 and Tfh B5 T cells. In addition, the MCMV
44 vector had adjuvant properties, contributing non-specifically through prolonged stimulation of
45 IFN-γ. *In vivo* neutralization of IFN-γ, but not IL-12 and IL-18, late in the course of MCMV, led
46 to loss of the adjuvant effect. Mechanistically, sustained IFN-γ from MCMV increased CD8α^{+}

dendritic cell numbers, and led to increased IL-12 production upon *Plasmodium* challenge. In addition, neutralization of IFN-γ before challenge reduced the polyclonal Teff response to challenge. Our findings suggest that, as protective epitopes are defined, an MCMV vectored booster can prolong protection through the innate effects of IFN-γ.

Authors' summary

Malaria represents a challenging target for vaccination. This is in part because of the requirement for CD4 T cell immunity in addition to the standard B cell responses current vaccines induce. However, human malaria vaccine approaches thus far have limited longevity of protection due to decay of T cell responses. This includes the most advanced malaria vaccine, a virus-like particle expressing one recombinant liver-stage antigen (RTS,S), and liver-stage parasites attenuated by radiation (PfSPZ), as well as live vaccination with drug-treatment. Our work seeks to prolong this protection using MCMV, a promising vaccine vector known to promote CD8 T cell responses. We observed that boosting the live malaria vaccine with MCMV including a *Plasmodium* antigen led to longer protection from *P. chabaudi* parasitemia, and can be used to promote maintenance of antigen-specific CD4 T cells. In investigating the mechanisms of the MCMV booster, we found that the cytokine IFN-γ is required for prolonged protection and enhances priming of the innate immune system for prolonged protection from malaria. Our research informs both the quest for a longer-lived malaria vaccine and that to understand mechanisms of protection from persistent infection.

Introduction

69 Compared to acute and localized infections, persistent systemic infections are the most challenging
70 vaccines to develop [1, 2]. Despite impressive progress for malaria vaccine development, and
71 using emerging approaches including live or attenuated parasites, and recombinant protein
72 constructs targeting different stages in the parasite life cycle, none of the current vaccine
73 candidates provides both highly effective and long-lived immunity. Both natural parasite infection
74 and malaria vaccines generate immunity to parasitemia on re-infection that wanes quickly, and
75 this is shown to be due to a progressive loss of specific T cells [3, 4]. Key insights to decay of
76 protection from persistent systemic infections has come from the study of immunity to parasite
77 infections with *Leishmania* and *Plasmodium spp.,* which decays over time in the absence of
78 infection [3, 5, 6]. Protection from recurrent infection in nature is likely mediated by sustained
79 generation of otherwise short-lived Th1 Teff while infection persists [7, 8]. We and others have
80 shown that both short-lived effector T cells and long-lived effector memory T cells are generated
81 in persistent infection. It is unclear if long-lived memory T cells (Tmem) play an important role,
82 or could be used to improve protection from potentially persistent systemic infections. Persistent
83 parasite infection, including *Leishmania major* or *P. chabaudi,* generate recirculating Tcm that do
84 not protect as well as activated Teff or Tem, defined as previously divided $CD4^{+}CD62L^{lo}$ Tem/Teff
85 [9], or distinguished as $CD127^{-}$ Teff and $CD127^{hi}$ $CD44^{hi}$ $CD62L^{lo}$ $CD27^{-}$ Tem [10]. In *P. chabaudi*
86 infection, we showed that inducing a pre-activated MSP1-specific B5 T cell receptor transgenic
87 (TCR Tg) T cell response, along with a B cell response to MSP-1 p19, before infection with *P.*
88 *chabaudi*, was an effective way to promote an effective reduction of the parasitemia of re-infection.
89 These data suggest an important role for effector T cells in protection. It should be noted that while
90 B5 T cells protect immunocompromised recipients from death, they do not eliminate parasite in
91 the absence of B cells [11]. By defining Teff as $CD127^{-}$, an early marker of T cell activation that

92 is transient and not present on Tem, we were able to determine that adoptively transferred Teff are
93 the most protective T cells in systemic, blood-stage *P. chabaudi* infection [8, 10]. However, short-
94 lived CD4 T cell immunity has been identified as the crucial variable resulting in short-term
95 protection from persistent *P. chabaudi* infection or vaccination [3, 12]. However, standard
96 vaccines do not generate durable Teff responses, leading to the problem at hand of what vaccine
97 vector to use to prolong protection, if the cell type that protects is short-lived.

98 Therefore, we investigated the potential of CMV to increase the duration of the T cell
99 response to effectively prolong vaccine-induced immunity to *Plasmodium* infection as a booster
100 vector. CMV has emerged as a promising long-lasting vaccine vector, for example, it provided
101 lasting immunity over a year against mucosal Simian Immunodeficiency virus (SIV) challenge in
102 Rhesus macaques [13]. CMV is a potent CD8 T cell-inducing vector with efficacy against SIV,
103 ebolavirus, tuberculosis, cancer and liver-stage malaria [14-18]. CMV infection can induce
104 sustained, or inflationary CD8 T cell responses with an effector memory phenotype. Th1-type
105 effector function is also generated [19-21], but the effect of persistent CMV on CD4 T cells is less
106 well understood. CMV also has non-specific effects suggesting a useful adjuvant effect of the
107 vector. For example, MCMV provides non-specific protection to *Listeria monocytogenes*, *Yersinia*
108 *pestis* and influenza virus, particularly in the latent phase of infection [22, 23]. Previous vaccine
109 studies all have used CMV in the priming phase of the vaccine response, and it has not been tested
110 as a vector for boosting existing responses, nor has it been studied extensively in the generation of
111 CD4 T cell responses. In addition, CMV generates effector/memory T cells, but the specific
112 phenotype has not been determined, and extending the duration of an effector response will be
113 critical to the fight against persistent infection.

114 In this study, we found that the MCMV vector boosted protection generated by a live
115 malaria vaccine against challenge infection with heterologous parasite. In addition to showing that
116 we can induce epitiope-specific effector T cells 40-60 days post-boost, we identified a significant
117 adjuvanting effect of boosting with MCMV. We showed that IFN-γ produced during the persistent
118 phase of MCMV increases CD8α$^+$ dendritic cell numbers. Upon challenge, MCMV boosted
119 animals had increased serum IL-12 and a larger CD4 polyclonal effector T cell response, which
120 were reduced by neutralization of IFN-γ before infection. This work informs our basic
121 understanding of the immunology and vaccinology of persistent infections, and suggests that
122 persistent stimulation of innate and adaptive mechanisms can promote persistence of protective
123 immunity.
124
125 **Results**
126 **MCMV as a vaccine vector with adjuvant properties against *P. chabaudi***
127 In order to evaluate an MCMV vaccine vector and observe vector- and *Plasmodium*-
128 specific CD4 T cell phenotypes, we generated an MCMV vector carrying the *P. chabaudi* MSP-1
129 B5 CD4 T cell epitope (MCMV-B5) using bacterial artificial chromosome (BAC) recombineering.
130 The B5 epitope was inserted in the intermediate early 1 locus with a linker to facilitate processing,
131 as diagrammed in **S1A Fig**. As MCMV has been shown to induce more sustained CD4 T cell
132 numbers in BALB/c, than in C57BL/6 mice [24], we developed a BALB/c system. Although *P.*
133 *chabaudi* MSP-1 B5 CD4$^+$ T cells prevent immunodeficient animals from dying, B5 T cells alone
134 do not affect *P. chabaudi* parasitemia significantly unless they are pre-activated, and in the
135 presence of parasite-specific B cells [11]. Several aspects of the virology and immunology of the
136 two constructs were compared for rigor of the study. The kinetics and tissue tropism of MCMV-

137 B5 infection was confirmed to be the same as the parental virus, MCMV-BAC using plaque assay
138 (**S1B Fig**) and PCR (**S1C Fig**). The virus is largely cleared by day 30, however low recrudescence
139 can be seen at later timepoints. Proportions of polyclonal $CD4^{+}CD127^{-}$ Teff, and $CD4^{+}$
140 $CD44^{hi}CD127^{hi}$ Tmem were similar for MCMV-BAC and MCMV-B5 at day 15 p.i. (**S1D Fig)**.
141 MCMV-specific $CD4^{+}$ T cells were identified using m78 peptide/I-A^{d} tetramers, using CLIP/I-A^{d}
142 as non-specific tetramer control, and MCMV-specific $CD8^{+}$ T cells were detected with the m45/D^{d}
143 -tetramer [20, 21]. Both MCMV-BAC and MCMV-B5 induced an MCMV m78-specific CD4 T
144 cell response at day 15 p.i. (**S1E Fig**). A large MCMV m45-specific CD8 T cell response to
145 MCMV-B5 was sustained near a million T cells per spleen from day 11 to 60 p.i. (**S1F Fig**).
146 MCMV is an excellent vaccine vector that showed early promise against liver-stage
147 malaria [16] and other infections fought by CD8 T cells. However, the mechanisms by which the
148 vector contributes to the adjuvanting protective effect are not well understood. To test for a
149 protective effect of the low chronic phase of MCMV infection on *P. chabaudi* challenge,
150 BALB/cByJ mice were infected with MCMV-B5 or MCMV-BAC or aged, and challenged 60 days
151 later with *P. chabaudi* AS, as shown schematically in **Fig 1A**. Groups given either MCMV-BAC
152 or MCMV-B5 had strongly reduced parasite growth upon *P. chabaudi* infection compared to a
153 primary infection age-matched control (**Fig 1B**). Pathology from malaria, as indicated by weight
154 loss, was also significantly inhibited by prior MCMV-BAC or MCMV-B5 infection (**Fig 1C**). This
155 strong, non-specific effect reduced parasitemia and pathology by about half, so not as effectively
156 as prior infection, or live vaccination [3].
157
158 **MCMV stimulates and maintains *Plasmodium*-specific T cell responses**

159 Using B5 TCR Tg T cells, we were able to distinguish the non-specific adjuvant effects
160 from epitope-specific effects on $CD4^+$ T cells [11]. To determine effects of the MCMV vector on
161 epitope-specific T cells, we adoptively transferred B5 Tg T cells (2×10^6) and infected the
162 recipients with MCMV-BAC or MCMV-B5, as illustrated in **Fig 2A**. The B5 CD4 T cell response
163 in the spleen 15 and 55 days post-MCMV infection was assessed by flow cytometry. The
164 proliferated B5 T cell (CTV^- $Thy1.2^+$) number was specifically increased by MCMV-B5, which
165 leading to a specific increase that lasted until day 55 (**Fig 2B**). MCMV-BAC infected mice also
166 maintained proliferated CTV^- B5 T cell numbers slightly above background to day 55. In order to
167 test the MCMV-driven generation of effector T cells, they were stained for the IL-7Rα (CD127),
168 which is downregulated on recently activated T cells. The majority of CTV^- B5 TCR Tg T cells
169 on day 15 are $CD127^-$ Teff (**Fig 2C**). On day 55, the fraction of Tmem increases, but a significant
170 number of Teff also are present, as clearly seen in the flow cytometry plot of B5 T cells recovered
171 at this timepoint (**Fig 2D**). In addition, we observed that MCMV-B5, but not MCMV-BAC,
172 specifically promoted the differentiation of MCMV-B5 epitope-specific GC Tfh ($CXCR5^{hi}PD\text{-}1^{hi}$,
173 **Fig 2E**).
174 We also detected some MCMV-specific CD4 T cell responses using MCMV m78 tetramer
175 at 11 and 60 days after MCMV-B5 infection (S2A **Fig**). MCMV-B5 infection induced MCMV
176 m78-specific $CD4^+$ T cell responses that persisted for two months (S2B **Fig**). Phenotypically,
177 MCMV vector-specific T cells were predominantly Teff (Tet^+ $CD127^-$) early in infection (day 11),
178 with re-upregulation of CD127 into a Tmem phenotype at day 60 (S2C **Fig**), similar to the B5-
179 specific response to MCMV-B5. Proliferation of transiently transferred B5 T cells in response to
180 MCMV-B5 was tested over various five-day windows. Congenic recipients (Thy1.1) were infected
181 with MCMV-BAC or MCMV-B5 or uninfected, and CTV-labelled CD4-purified B5 TCR Tg T

182 cells were adoptively transferred for the last five days of infection, testing presentation of B5
183 peptide between days 5-10, 25-30, or 55-60 of MCMV infection. Splenocytes were analyzed for
184 proliferation (%CTV-) of B5 T cells in each experimental window (**S2D Fig**). The MCMV-B5
185 vector, and not the MCMV-BAC control, led to strong specific proliferation of epitope-specific
186 B5 Tg T cells during acute infection (days 5-10) (**S2E Fig**). Despite the presence of B5 TCR Tg
187 Teff on day 55, there was no detectable proliferation in this assay at later timepoints. This may be
188 due to background proliferation, even in uninfected animals.
189

190 **MCMV boosts long-term protection of live malaria vaccine**

191 As the protection of malaria vaccines tested in mice and humans decays after one to two
192 years [25, 26], we sought to test a vaccine booster strategy to prolong immunity. *Plasmodium spp*.
193 infection followed by drug treatment is an effective vaccination protocol in C57BL/6 mice, and
194 also in human studies; however, this protection shows measurable decay by day 200 in mice [3,
195 27]. Using the protocol published by Freitas do Rosario et al, where mice are infected with *P.*
196 *chabaudi* AS followed by sub-curative dose of chloroquine each time parasitemia reaches 1%, we
197 tested sterilizing immunity with heterologous reinfection (**S3A Fig**). This experiment confirmed
198 that *P. chabaudi* infection induced sterilizing immunity for two months, and that a measurable
199 decay in protection was evident by day 200 in BALB/c mice (**S3B Fig**), as in B6. We also
200 confirmed that there was not a measurable decay in antibody concentration between 2 and 6.5
201 months p.i., as shown previously in B6 mice (**S3C Fig**), leading us to test a known T cell-response-
202 promoting vector to attempt to prolong T cell responses and protection through as yet unknown
203 adjuvant effects.

204 To test the potential of an MCMV-based booster vaccine, mice were vaccinated with live
205 *P. chabaudi* AS infection followed by sub-curative doses of chloroquine and then boosted with
206 MCMV-BAC or MCMV-B5 140 days later, as schematically depicted in **Fig 3A**. As vaccine-
207 induced protection decays by day 200, we tested MCMV boosters for protection from heterologous
208 re-infection with *P. chabaudi* AJ at day 200, which corresponds to 60 days after boosting. This
209 timing was chosen on the basis that neither immunity nor the T cell response to live vaccination
210 has completely decayed by day 120 [3, 12], and that the MCMV infection is below detectable by
211 day 60 [24], though we expected it to show prolonged stimulatory capacity at this timepoint [22].
212 Age- and sex-matched *Plasmodium*-vaccinated mice, with or without the MCMV-booster, were
213 challenged with heterologous *Plasmodium* infection. The booster prolonged live vaccine induced
214 protection, as evidenced by the data shown in **Fig 3B** that mice that were boosted with MCMV
215 had a lower parasitemia on challenge on day 200 post-vaccination (p.v., average of 0.06%, or
216 0.05% without or with the B5 epitope, respectively), on day 4 post-challenge (p.c.), than
217 vaccinated mice challenged without boosting (1.57% on day 4 p.c., and 0.5% on day 6 p.c.). The
218 boosting effect does not require the B5 epitope in a significant way, which is not surprising, B5
219 CD4 T cell epitope was included as a way to track specific T cells, not to protect as a single epitope.
220 Heterologous parasite-specific serum antibody was measured by ELISA at day 7 p.c. (**Fig 3C**). As
221 previously reported parasite-specific IgG responses remain stable up to day 200 post-live
222 vaccination [3], ELISA showed that levels of *P. chabaudi* AJ-specific serum IgG in the first week
223 of challenge were not altered by the MCMV booster (**Fig 3C**). The boost was specifically chosen
224 to promote T cell responses to support the ongoing antibody response generated by the live
225 vaccine. In summary, *Plasmodium* vaccination efficacy, but not serum antibody, fades with time,
226 and boosting with MCMV prolonged protection.

227

228 **MCMV can boost parasite-specific T cell immunity induced by live malaria vaccine**

229 CMV is a promising CD8 T cell-inducing vaccine vector and generates Tem and
230 inflationary effector T cells [20, 28]. Less is known about CD4 T cell phenotypes in response to
231 MCMV [20], and the potential for continuous generation of phenotypic effector CD4 T cells in the
232 persistent phase is not well understood. In order to determine if MCMV-B5 boosted *Plasmodium*-
233 specific CD4 T cell responses, B5 CD4 TCR Tg cells (Cell Trace Violet (CTV)-labelled) were
234 adoptively transferred into congenic recipients (Thy1.1 BALB/cByJ), which were then immunized
235 with live *P. chabaudi* vaccine, and boosted with MCMV-B5 or MCMV-BAC at day 140 p.v. (**Fig**
236 **4A**). B5 T cell effector and effector memory phenotype and cytokine responses were quantified at
237 day 200 p.v.. Using MCMV-B5, as a booster to the live malaria vaccine specifically and
238 significantly increased the numbers of divided B5 TCR Tg T cells ($CD4^{+}CTV^{-}Thy1.2^{+}$) present
239 on day 200 p.v., while MCMV-BAC did not (**Fig 4B**). Therefore, more transferred B5 T cells
240 survived to day 200 after MCMV-B5 boost. B5 TCR Tg cells are not detectable after 200 days in
241 the absence of parasite [8]. The MCMV-B5 boost 60 days earlier specifically increased the
242 numbers of both $CD127^{-}$ B5 Teff and $CD127^{hi}$ B5 Tmem present at day 200, while MCMV-BAC
243 did not increase B5 T cell numbers (**Fig 4C**). Among Tmem subsets, the number of both $CD27^{+}$
244 and $CD27^{-}$ effector memory T cells ($CD44^{hi}CD127^{hi}CD62L^{lo}$, Tem) were significantly higher in
245 MCMV-B5 boosted mice, while central memory ($CD62L^{hi}$ Tcm) were not increased by MCMV
246 boost (**Fig 4D**). In addition, the MCMV-B5 booster specifically generated or maintained functional
247 B5 T helper type 1-type cells, as shown by their production of IFN-γ (**Fig 4E**), TNF (**Fig 4F**) and
248 IL-2 (**Fig 4G**) at day 200. This data show that the vector generated well-presented epitopes, and

249 could be used as a booster vaccine for T cells. In addition, the vector induced effector T cells for
250 a longer time than reported for acute stimulation, in addition to making Tem.
251
252 **IFN-γ, but not IL-12 and IL-18, induced by MCMV, is associated with protection from *P.***
253 ***chabaudi* infection**
254 As we had observed a protective effect by the MCMV-BAC, we took the opportunity to
255 understand mechanisms explaining the observed benefits of using this virus as a vaccine vector in
256 addition to the ability to present T cell epitopes and generate Teff. To determine if cytokines
257 induced by long-term MCMV infection are mechanistically responsible for promoting protection
258 from heterologous challenge, we used neutralizing antibodies to test the roles of IFN-γ, as well as
259 the combination of IL-12 and IL-18, in the period before challenge after 40 days of MCMV
260 infection. IFN-γ was neutralized starting on day 34 of MCMV-BAC infection, and before *P.*
261 *chabaudi* challenge, as shown schematically in **Fig 5A**. *In vivo* neutralization of IFN-γ after
262 MCMV, but before *P. chabaudi* infection was associated with a substantial loss of protection
263 against *P. chabaudi* challenge. The mice treated with anti-IFN-γ before infection had significantly
264 higher parasitemia compared to isotype-treated controls previously infected with MCMV (**Fig 5B**).
265 The level of parasitemia in mice receiving neutralizing antibody is similar to a first infection
266 suggesting that all or most of the reduction due to MCMV is due to IFN-γ. The effect of
267 neutralizing MCMV-induced IFN-γ on challenge is also reflected in increased pathology, as
268 measured by weight loss (**Fig 5C**), and hypothermia (**Fig 5D**). To determine if there is an effect of
269 MCMV persistence-induced IFN-γ on the T cell response to challenge, the polyclonal $CD4^+$ T cell
270 phenotype was examined on day 15 post-challenge with *P. chabaudi.* Surprisingly, there was a
271 significant reduction in responding $CD4^+$ Teff after pre-treatment with anti-IFN-γ (**Fig 5E**).

272 Evaluation of serum cytokines in MCMV infected animals showed IL-12p40 production
273 throughout MCMV infection (**Fig 5F)** that is increased upon *P. chabaudi* challenge (**Fig 5G**).
274 Strikingly, IL-12 p40 production on days 7, 8 and 15 p.c. as well as TNF, CXCL-9 and CXCL-10
275 on day 7 p.c. were significantly reduced by neutralization of IFN-γ for six days before challenge
276 while IL-10 level was increased at 7 days p.c. (**Fig 5H)**. We also measured other cytokines
277 including IL-6, IL-15, IL-18, IFN-α and IFN-β, which are known to be produced during MCMV
278 infection to see if they were affected by neutralization of IFN-γ but did not see significant
279 differences at these time points.

280 To investigate potential direct effects of neutralizing IFN-γ on challenge parasitemia due
281 to persisting antibody and determine the role of persistent IFN-γ induced by MCMV in protection,
282 we examined the effect of anti- IFN-γ clone H22 on *P. chabaudi* infection with or without an
283 earlier dose of MCMV (**S4A Fig**). We found that administration of neutralizing antibody up to 2
284 days before infection with *P. chabaudi* does not have a significant measurable effect on peak
285 parasitemia (**S4B Fig**), while it does affect parasitemia significantly, as above, if MCMV is given
286 before infection (**S4C Fig**). To determine if neutralizing levels of antibody remained in the serum
287 during challenge, we developed an assay to test induction of CXCL10, which is induced in
288 macrophages by IFN-γ. CXCL10 mRNA was measured after culture of RAW 264.7 cells with
289 serum from mice before challenge (d40, **S4D Fig**), and on day 7 post *P. chabaudi* challenge with
290 or without prior anti-IFN-γ administration (**S4E Fig**). We found no detectable change for the
291 relative CXCL10 mRNA level with Raw 264.7 cells cultured with d40 or d47 serum, though there
292 was a trend suggesting antibody was there. Adding recombinant IFN-γ (rIFN-γ) to the assay
293 allowed detection of neutralizing antibody. In this assay, a reduced level of CXCL10 mRNA was
294 detectable in the presence of serum from 2 days after anti-IFN-γ (**S4F Fig**) and day 7 *P. chabaudi*

295 challenge (**S4G Fig**). Therefore, though neutralizing antibody does remain in the system during *P.*
296 *chabaudi* challenge, we conclude that the large effect of blocking IFN-γ after MCMV, and before
297 challenge, is mostly due to inhibition of MCMV-induced not *P. chabaudi*-induced IFN-γ.
298 Therefore, we investigated the mechanisms of this strong effect.

299 As IL-12 and IL-18 can induce IFN-γ from NK cells or previously stimulated T cells, we
300 queried their role in induction of IFN-γ by MCMV, but did not find any effect of blocking IL-12
301 and IL-18 together in the time period before challenge on protection from *P. chabaudi* parasitemia
302 or pathology by the MCMV vector (**S5 Fig**).

303 To explore the effect of IFN-γ on persisting epitope-specific T cells and the innate response in the
304 context of late MCMV infection, we adoptively transferred CTV-labelled B5 TCR Tg T cells into
305 Thy1.1 mice and then infected them with MCMV-B5, as illustrated in **Fig 6A**. IFN-γ was
306 neutralized on days 44-48 of MCMV infection. Blocking IFN-γ induced by MCMV-B5 infection
307 did not change the number of CTV^- B5 T cells at day 50 p.i. (**Fig 6B**). IFN-γ also did not affect
308 the phenotype, as measured by the fraction of both Teff and Tmem (**Fig 6C**), or representation of
309 Tmem subsets, as defined by CD27 and CD62L expression (**Fig 6D**). B5 T cells induced by
310 MCMV-B5 are mostly memory T cells, with a fraction of effector T cells that is larger than that
311 seen on day 60 of *P. chabaudi* infection [8]. A panel of innate cell markers showed that after IFN-γ
312 neutralization on day 50 post-MCMV infection, the number of $CD8\alpha^-$ DCs ($CD3^-$
313 $CD11c^{hi}MHCII^{hi}$) remained constant while the number of $CD8\alpha^+$ DCs showed a trend towards a
314 reduction (**Fig 6E**). The level of IL-12p40 in the serum on day 50 post-MCMV infection was
315 significantly reduced in the group that received IFN-γ neutralizing antibody compared to isotype
316 (**Fig 6F**). Splenic $CD8\alpha^+$ DCs are the major producers of IL-12p40 in response to systemic stimuli
317 [29].

318

319 **IFN-γ generated by the MCMV booster drives prolonged protection of live malaria vaccine**

320 Given the ability of MCMV to prolong protection from challenge and to promote IL-12 in
321 an IFN-γ dependent manner, we tested mechanisms of the prolonged protection. Mice were
322 vaccinated and then boosted with MCMV at day 140, as in **Fig 4**, with adoptive transfer of B5 T
323 cells to determine the effect on vector-driven T cells. B5 T cell recipients were immunized with
324 live malaria vaccine and boosted with MCMV-B5 at day 140 p.v., as illustrated in **Fig 7A.** Half of
325 these animals received neutralizing antibody to IFN-γ, or isotype control antibody, days 194-198
326 p.v. (days 54-58 after the MCMV-B5 booster). T cell and antigen-presenting cell phenotypes were
327 assessed at day 200 after malaria immunization, in the absence of challenge. Live *P. chabaudi*
328 vaccination plus MCMV-B5 booster tended to increase survival of B5 T cells compared to live
329 vaccine alone, as above, though this effect did not reach significance in this experiment (**Fig 7B**).
330 Neutralization of IFN-γ did not have an effect on specific malaria vaccine-driven, MCMV-B5
331 boosted B5 T cell numbers, or the composition of Tmem subsets (**Fig 7C**). These data indicate that
332 IFN-γ does not promote T cell survival or Tem differentiation directly, after MCMV-B5 boost,
333 supporting the specific effect of MCMV-B5 epitope on the specific T cell responses. Staining for
334 innate cell types, $CD11c^{hi}$ dendritic cells (DC) were found to be increased by MCMV boost (**Fig**
335 **7D**). Furthermore, *in vivo* neutralization of IFN-γ significantly reduced the DC numbers compared
336 to isotype control (**Fig 7D**). This innate effect was seen most strikingly in the $CD8\alpha^{+}$ DC ($CD3^{-}$
337 $CD11c^{hi}MHCII^{hi}CD8\alpha^{+}$) population (**Fig 7E**). We also assessed NK cells, and monocyte derived
338 subsets including monocytes, macrophages and inflammatory monocytes to see if their numbers
339 or activation marker expression were affected by neutralization of IFN-γ, but did not see other
340 significant differences **(S6 Fig)**. Blocking IFN-γ after vaccination and the MCMV booster caused

341 a trend towards a reduced serum level of IL-12p40, though this did not reach significance, as it did
342 in MCMV infection alone on day 50 (**Fig 7F**). To test the role of MCMV booster-induced IFN-γ
343 in prolonging vaccine-induced protection, mice were vaccinated and then boosted with MCMV-
344 BAC at day 140, as above in **Fig 3**, and as shown schematically in **Fig 7G**. The control groups
345 either had no live vaccine and no MCMV or no vaccine and then MCMV only. Prior to
346 heterologous challenge with *P. chabaudi* AJ at day 200, vaccinated mice with MCMV boost
347 received IFN-γ neutralizing antibody, or isotype control, at days 194-198 p.v. (54-58 days post-
348 MCMV booster). MCMV boosting live vaccination showed significant protection against weight
349 loss (**Fig 7H)** and parasitemia (**Fig 7I)** compared to the adjuvanting effect of MCMV or
350 unvaccinated control mice. Blocking IFN-γ before challenge significantly reduced the booster
351 effect of the MCMV-BAC on protection at day 200 (**Fig 7J**). This was measured as a significant
352 increase in parasitemia in the IFN-γ neutralized animals (0.4%), compared to the isotype group
353 (0.09%), on day 5 post-challenge. While this is clearly a non-specific effect, as there is no B5
354 epitope here, polyclonal T cell phenotyping on day 15 post-challenge again showed that blocking
355 IFN-γ before reinfection significantly reduced the fraction of Teff generated during *P. chabaudi*
356 challenge, and was associated with higher parasitemia, suggesting a role for antigen presentation
357 during challenge that was not tested here (**Fig 7K**). Serum levels of *P. chabaudi* AJ-specific IgG
358 increased after challenge, but there was no significant difference from neutralization of IFN-γ (**Fig**
359 **7L**). Collectively, these data suggest a novel innate pathway where viral vector-induced IFN-γ
360 drives an increase in CD8α+ DCs, which promote increased protective IL-12 and Teff upon
361 challenge. We have identified two novel mechanisms of adjuvanting supporting the promise of
362 CMV-based vaccines, and defined a promising line of research for prolonging protection from

363 *Plasmodium* infection. Testing the full capacity of this strategy would require the identification of
364 more protective T cell epitopes.
365
366 **Discussion**
367 Alternative high-efficacy approaches for all malaria vaccine continue to be developed, but
368 little engineering has been focused on increasing longevity. These data show significant promise
369 for use of chronic vaccination to prolong the current short half-life of vaccines against systemic
370 infections requiring CD4 T cell memory. In summary, we demonstrated an adjuvant effect
371 dependent on the MCMV vector-induced IFN-γ that enhances CD8α^+ dendritic cell numbers, and
372 IL-12 production upon challenge. In addition, we demonstrate two basic mechanisms for the
373 extension of protection provided by the chronic MCMV booster to a typical short-lived malaria
374 vaccine. The MCMV vaccine-expressing a malaria epitope prolongs survival of epitope-specific
375 CD4 Teff and Tem. Polyclonal effector T cell numbers also increase when challenge occurs in the
376 presence of MCMV-induced IFN-γ, suggesting that the underlying mechanism of protection from
377 challenge is an increased Th1 response to *Plasmodium* due to increased IL-12 downstream of
378 higher dendritic cell numbers at the time of challenge.
379 We observed a strong adjuvant effect of the MCMV vector itself on *P. chabaudi* infection.
380 The effect of MCMV alone reduced *P. chabaudi* challenge parasitemia by about one half. The
381 adjuvant effect alone also drove a significant fraction of the prolonged protection seen from using
382 the MCMV vector in a boosting strategy, as demonstrated by neutralizing the IFN-γ induced by
383 MCMV-BAC before challenge. MCMV and gamma herpesvirus 68 also have an adjuvant effect
384 against influenza virus and *Listeria monocytogenes*, but not West Nile virus [22, 23], indicating
385 some specificity. This specificity may be due to latency. Gamma Herpesvirus 68 with a point

386 mutation in ORF73, a gene required for latency, showed reduced protection from *Listeria*, and also
387 reduced IFN-γ levels and chronic macrophage activation. HSV-1 and Sindbis viruses, which do
388 not establish latency, did not have this protective effect [22]. MCMV-induced cross-protection
389 against influenza also lasts through early and established (5-12 weeks), but not long-standing (9
390 months) MCMV latency. Production of IFN-γ during the latent phase of infection has also been
391 implicated in MCMV-induced protection to *Listeria* and *Yersinia* [22], influenza; which was
392 abrogated in IFN-γ deficient mice [23]. Our work extends these findings mechanistically by
393 showing that neutralizing IFN-γ late in MCMV infection reduced the number of CD8α^+ dendritic
394 cells in the spleen, and reduced the amount of some cytokines and chemokines IL-12, CXCL-9
395 and CXCL-10 and the number of CD4 Teff, but increased IL-10 cytokine level on challenge. While
396 we did not specifically test for latency, our vectors showed similar kinetics and outcomes to
397 previous studies suggesting infection with our vectors would be latent in our mouse model by day
398 40 [24]. Mechanisms of this protection had not been specifically established.

399 Decay of immunity, and failure to maintain *Plasmodium*-specific CD4 T cells make the
400 development of an effective and long-lived malaria vaccine challenging. Both natural immunity to
401 the parasite, and vaccines, generate immunity that decays due to a progressive loss of malaria-
402 specific T cells limiting long-lived protection [3, 4, 30, 31]. To our knowledge, there are no current
403 vaccine formulations that drive long-lived CD4 T cell responses [2, 32]. Therefore, the potential
404 of CMV to induce a prolonged T cell response with the desired phenotype was used to extend
405 vaccine protection. In this study, a two-step vaccine strategy that first induces a long-lived
406 protective antibody response, and then boosts with an MCMV strategy was chosen for the potential
407 to extend effector/memory CD4 T cells responses over a longer period to prolong protection. While
408 the protective T cell epitopes are not well defined, using a parasite derived CD4 T cell epitope

409 allowed us to test this strategy in a pre-clinical setting. Boosting with the MCMV vector did
410 prolong the protection generated by the live infection and-drug cure malaria vaccine as evidenced
411 by reduced challenge parasitemia after boost. The data show that animals that received live malaria
412 vaccination became susceptible to heterologous re-infection by day 200 p.v., while the MCMV-
413 B5 boost maintained the protection seen at day 60 until day 200. All malaria vaccines tested in
414 human studies thus far, including the most advanced vaccine RTS,S, show insufficient longevity
415 of protection [25].

416 CMV induces a robust and long-lasting T cell response including both effector and memory
417 components [20, 33]. Hansen et al. showed recently that RhCMV-expressing *Plasmodium*
418 *knowlesi* antigens, generated a parasite antigen-specific immune response that delayed parasite
419 growth upon sporozoite challenge via generation of CD8 T cell responses [16]. However, whether
420 an MCMV vector could be used to boost pre-existing specificities has not been tested, and only a
421 few studies have investigated CD4 T cell responses to MCMV [34]. Here we show that the MCMV
422 vector can be used to specifically boost CD4 epitope-specific effector T cell responses, which is
423 one of the primary gaps in our current malaria vaccine arsenal. Both CD4 Teff and Tmem
424 phenotypes are generated in *P. chabaudi* infection, and both promote protection [8, 10]. Here, we
425 observed that MCMV-B5 increased epitope-specific T cells, and specifically generated GC-Tfh
426 and promoted maintenance of the Tem phenotype and effector functions (IFN-γ, TNF and IL-2)
427 past day 200. CD4 T cells are crucial for protective immunity to *P. chabaudi* as they produce
428 cytokines that both promote phagocytosis and B cell help [35]. Our previous findings revealed the
429 power of Teff in protection from persistent *P. chabaudi* with help from B cells. Adoptive transfer
430 of B5 effector CD4 T cells reduced the peak of *P. chabaudi* parasitemia by half [10]. While
431 memory T cells are less effective, $CD27^-$ TemL do reduce parasitemia, and are the most protective

432 memory phenotype. In this study, we showed that the MCMV-B5 vector specifically activated and
433 maintained both adoptively transferred epitope-specific T cells and MCMV-specific $CD4^+$ T cells
434 over 2 months. Interestingly, Teff were clearly present among the few m78-Tetramer MCMV-
435 specific CD4 T cells over 2 months, but did not reach significant levels compared to uninfected
436 controls. This may reflect the small number of cells detected, and so we used the B5 TCR Tg to
437 test for MCMV-induced proliferation at late time points, however this assay had high background.
438 Consistent with this, MCMV-B5 maintained both Teff and the potentially protective late effector
439 memory phenotype T cells generated by *P. chabaudi* infection. While we do not present evidence
440 here that the protection provided is due to increased survival of B5 T cells, their numbers are
441 boosted at a timepoint when live vaccine induced T cells and protection would otherwise decay,
442 though antibody levels remain constant. It should be noted that the B5 specificity is not especially
443 potent in protection, as the effect of this one specificity is only seen in immunocompromised
444 animals. CD8 T cells specific for some MCMV loci are given to inflationary activation, even after
445 15 weeks of MCMV infection [36]. The locus where B5 is expressed, IE1, can be a memory
446 inflation inducing locus for CD8 T cells [37]. CD4 T cell responses to MCMV are even less well
447 understood. Therefore, additional T cell epitope discovery in this field will aid in the long-term
448 goal of developing durable vaccine induced protection.

449 The MCMV vector increased $CD8\alpha^+$ DCs and IL-12 both before challenge, and in response
450 to the parasite. Induction of IL-12 upon *P. chabaudi* challenge was reduced in the context of prior
451 neutralization of IFN-γ. Considering that $CD8\alpha^+$ DCs are a key source of IL-12 production in many
452 infections [38], and also present antigen to T cells upon infection, the reduced IL-12 level in
453 response to *P. chabaudi* challenge after IFN-γ neutralization could be directly linked to the change
454 in Teff cell numbers seen. While IL-12 is more commonly associated with stimulating IFN-γ

455 production, IL-12 production by DC and macrophages can also be promoted by IFN-γ present in
456 the milieu, representing a positive feedback mechanism [39, 40]. Therefore, prolonged IFN-γ
457 appears to be maintaining CD8α$^+$ DCs, an IL-12 producing cell type, suggesting a novel
458 mechanism for this feedback. As IL-12 deficient mice have higher *P. chabaudi* parasitemia than
459 WT [41], or Ifng deficient animals [42], the reduced IL-12 response during challenge is likely to
460 explain the reduced control of parasites seen upon neutralization of IFN-γ. While more research
461 will be required to establish if the increase in dendritic cells late in MCMV infection is sufficient
462 to drive the increased IL-12 response or the increase in Teff upon challenge, the increase of CD8α$^+$
463 DCs supports this interpretation.

464 Prior work has shown that giving *P. chabaudi*-infected mice recombinant IFN-γ increased
465 the number of polyclonal CD4 Tem, and also prolonged heterologous immunity. In our system,
466 generation and maintenance of Tem is epitope specific, and not affected by blocking IFN-γ
467 generated during MCMV infection. Our previous work showed that both memory T cell
468 differentiation and prolonged infection contribute to maintenance of Tem numbers in *P. chabaudi*
469 infection [10]. It remains to be proven whether the MCMV-BAC driven increase in DCs, and/or
470 priming of them to respond/present antigen, leads directly to enhanced responsiveness of parasite
471 specific T cells/expansion and clearance of parasite by Th1-promoted macrophage activation and
472 Tfh-promoted antibody production. It is also possible that antigen presentation and Th1 response
473 are reduced with the presence of detectable anti-IFN-γ auto-antibody [43]. Exploring this
474 hypothesis to determine potential effects of anti-IFN-γ antibody, we found that administration of
475 neutralizing antibody up to 2 days before infection with *P. chabaudi* does not have a significant
476 effect on peak parasitemia, though there may be a trend towards increasing parasitemia. Indeed, in
477 Meding et al, where IFN-γ was neutralized during the infection, the change in parasitemia was

478 very small [42], similar to the effects of anti-IFN-γ seen on primary infection in our study. There
479 is a clear reduction of these IFN-γ-inducible chemokines (CXCL9 and CXCL10) in the serum
480 upon infection after anti-IFN-γ. This suggests that anti-IFN-γ directly or indirectly reduces their
481 production in response to the parasite. An indirect example would be that these chemokines can
482 be made by DCs, the reduction of IFN-γ induced chemokines could reflect the changes on DC
483 number that we have documented downstream of MCMV. Our results show that although
484 neutralizing antibody persists into the challenge phase, the largest effect of anti-IFN-γ after
485 boosting, requires MCMV-induced IFN-γ, and is not a direct effect on parasitemia.

486 Neutralization of IFN-γ led to a loss of the extended protection provided by MCMV
487 boosting and protection from *P. chabaudi* infection. Teff were reduced on challenge after IFN-γ
488 neutralization, which is particularly striking given the increase in parasite in anti-IFN-γ pre-treated
489 animals. IFN-γ production has been previously reported in MCMV and HCMV infection during
490 the period coinciding with latency [23]. Data from our laboratory and others establishes that IFN-γ
491 expression during persistent *P. chabaudi* infection, or recombinant IFN-γ also promote protection
492 from heterologous re-infection at day 200 [12, 44]. It was also reported that rIFN-γ increased the
493 number of polyclonal Tem at day 200 after *P. chabaudi* infection [44].

494

495 We have used basic knowledge of T cell differentiation in *P. chabaudi* infection to reverse
496 engineer a novel chronic vaccine strategy. We demonstrate a method and a mechanism to prolong
497 protection by a live malaria vaccine, which alone is short-lived, due to a loss of specific T cells.
498 Our work is novel as it indicates that MCMV works as a booster for CD4 T cell responses both by
499 maintaining specific effector and effector memory T cells and also as an adjuvant driving
500 protective IFN-γ production. The increase in dendritic cell numbers and increased IL-12 induced

501 by MCMV, together with and a trend towards increased Th1 cytokines upon challenge, suggest
502 that ultimately, a stronger T cell response to parasite explains the prolonged protection. This
503 strategy has the potential to resolve the major issue of short-lived protection generated by malaria
504 vaccines, as well as help understand how natural immunity could be prolonged. There are safety
505 issues to work out before CMV vectors could be used in humans. However, superinfection, the
506 ability to re-infect CMV carriers, and a varied T cell response are two benefits of this approach
507 [45, 46]. Further understanding of the mechanisms of this exciting new model could lead to more
508 rapidly translatable tools in the quest to prolong immunity to persistent or recurrent pathogens
509 without introducing another pathogen. This could be applicable to malaria, a disease that kills up
510 to half a million people a year; as well as other persistent or recurrent pathogens.
511

512 **Materials and methods**

513 **Ethics statement**

514 All experiments were carried out according to protocol approved by the University of
515 Texas Medical Branch Institutional Animal Care and Use Committee (IACUC).
516

517 **Mice, Parasites and Immunization**

518 All mice used in our study were maintained in the UTMB animal facility under specific
519 pathogen-free conditions with access to food and water *ad libitum*. Recipient Thy1.1 BALB/cByJ
520 were backcrossed to BALB/cJ (N4; The Jackson Laboratory, Bar Harbor, ME). B5 T cell receptor
521 transgenic (TCR Tg), which recognizes a peptide from merozoite surface protein-1 (MSP-1; 1157-
522 1171, ISVLKSRLLKRKKYI/I-E^d) was backcrossed to BALB/cJ (N10). B5 TCR Tg mice, and *P.*
523 *chabaudi chabaudi* AS stocks, were a kind gift from J. Langhorne (Francis Crick Institute, London,

524 UK). *P. chabaudi* AJ (MRA-740, a cloned line that is highly related but heterologous to AS [47,
525 48] was purchased from BEI Resources, formerly MR4. B5 TCR Tg mice were typed using
526 primers Vα2, 5′-gaacgttccagattccatgg-3′ and 5′-atggacaagatcctgacagcatcg-3′, and vβ8.1, 5'
527 cagagaccctcaggcggctgctcagg-3′ and 5′-atgggctccaggctgttctttgtggttttgattc-3′ [8]. Both male and
528 female recipients were used, however no sex differences in infection were noted. All adoptive
529 transfer experiments were done using age- and sex- matched recipient and donors.

530 For infection and drug cure vaccination, the protocol was performed as previously
531 documented in mice and humans [3, 27]. Six- to nine-week old mice were infected (10^6 *P.*
532 *chabaudi)* and treated with two subsequent noncurative doses of chloroquine (10 mg/kg body
533 weight/day; Sigma-Aldrich), when parasitemia reached 1-2% of erythrocytes. Parasites were
534 counted by light microscopy in thin blood smears stained with Giemsa (Sigma-Aldrich, St. Louis,
535 MO). Parasitemia was monitored by microscopic examination of thin blood smears from the tail.
536 Thin blood smears were stained with Giemsa (Ricca chemical company, Arlington, TX), and
537 parasites were counted by light microscopy.

538

539 **Construction of MCMV and viral infection**

540 A vaccine vector, MCMV-K181-B5, was generated as follows. MCMV-K181-Perth was
541 genetically modified to carry the MHC II-E^d-restricted B5 epitope (ISVLKSRLLKRKKYI) from
542 the *Plasmodium chabaudi* Merozoite Surface Protein MSP1 (1157–1171) in frame with the C-
543 terminus end of the MCMV IE1 gene (**Fig S1 A**). The B5 epitope was inserted into the MCMV-
544 K181 genome using bacterial artificial chromosome recombineering, as described previously [49].
545 The resulting virus was denoted MCMV-B5. Mice were infected by injecting $5x10^3$ PFU of

546 salivary gland-propagated MCMV-B5 virus or the parental virus, MCMV-K181-Perth (MCMV-
547 BAC). Viruses were injected i.p. in 0.2ml of PBS.
548
549 **Virus quantification**
550 MCMV-B5 or MCMV-BAC viral copy number of CMV/β-actin ratios were determined in
551 different organs in infected BALB/cJ mice. DNA was purified from tissue (liver, lung, and salivary
552 gland) using the Gentra Puregene Kit (Qiagen, Valencia, CA) following manufacturer's
553 instructions. All tissues were stored at -80°C in PBS for DNA, or Trizol (Thermo Fisher Scientific,
554 Carlsbad, CA) for RNA purification, until sample processing. qPCR was performed with 50 ng of
555 purified DNA. Specific primers for MCMV immediate early (IE1) gene (NCBI Accession No.
556 M11788) 5-tca gcc atc aac tct gct acc aac-3 and 5-gtg cta gat tgt atc tgg tgc tcc tc-3 and for murine
557 β-actin (Accession No. M12481) 5-gct gta ttc ccc tcc atc gtg -3 and 5-cac ggt tgg cct tag ggt tca-
558 3. Serial dilutions of a control plasmid were used to generate a standard curve for both MCMV-
559 IE1 and β-actin, as described previously, and qPCR of viral DNA has been shown to correlate
560 quantitatively with the plaque assay throughout the viral infection [50]. All sample measurements
561 were performed in triplicate. Real time PCR (VIIA, AB Biosystems, Life Technologies, Carlsbad,
562 CA).
563
564 **Cell culture with serum, RNA isolation and real-time PCR analysis**
565 RAW264.7 macrophage-like cell line was cultured in RPMI medium (Gibco)
566 supplemented with 10% (v/v) fetal bovine serum and antibiotics (100 U/ml penicillin and 100
567 lg/ml streptomycin), Sodium Pyruvate (100x, Gibco), 45% D-Glucose (100x, Sigma), L-glutamine
568 (100x, Corning) at atmosphere of 5% CO2. RAW264.7 cells were incubated with sera form IFN-

569 γ neutralizing mice with or without recombinant IFN-γ for 24h. Total RNA was extracted with
570 Direct-Zol RNA reagents (Zymo research, R2025) as described by the manufacturer. cDNA was
571 synthesized from total RNA using the iScript cDNA Synthesis kit (Bio-Rad). Real-time PCR was
572 performed with cDNA using the SYBR Green Supermix (Bio-Rad). The β-actin gene was used for
573 normalization. Relative changes in gene expression were calculated using the comparative
574 threshold cycle (Ct) method. The following primers were used: CXCL-10 5'-
575 cctgctgggtctgagtggga-3' and 5'-gataggctcgcagggatgat-3'; β-actin 5-gctgtattcccctccatcgtg-3 and 5-
576 cacggttggccttagggttca-3.
577
578 **Adoptive transfers and *in vivo* studies**
579 MACS-purified $CD4^+$ T cells from young, uninfected B5 TCR-Tg mouse spleens (Miltenyi
580 San Diego, CA) were labelled with cell trace violet (CTV) and adoptively transferred (2×10^6) into
581 Thy1.1 congenic mice. For cytokine neutralization, three doses of anti-IFN-γ antibody (H22, 0.5
582 mg) or isotype control antibody (PIP, 0.5 mg); or a combination of anti-IL-12p40 (C17.8, rat
583 IgG2a, 300 μg) and anti-IL-18 antibody (YIGIF74–1G7, control Rat IgG2a, 200 μg) were given,
584 every other day. All *in vivo* antibodies were from BioXCell (Lebanon, NH).
585
586 **Flow cytometry**
587 Single-cell suspensions from spleens were prepared at the indicated time points after infection in
588 HBSS) with HEPES (Thermo Fisher Scientific, Waltham, MA) using gentleMACS (Miltenyi, San
589 Diego, CA) and incubated in RBC lysis buffer (eBioscience, San Diego, CA). Single cells were
590 stained extracellular in PBS, 2% FBS, and 0.1% sodium azide with antibodies. For T cells: anti-
591 CD127 (A7R34), anti-PD-1 (RMP1-30), anti-CD62L (MEL-14), CD4 (RM4-5), (anti-CD90.2

592 [30-H12], anti-CD44 [IM7], and anti-CD27 [LG-7F9]) (all from eBioscience/Invitrogen and
593 Biolegend, San Diego, CA). Phenotype of polyclonal $CD4^+$ T cell subsets and *Plasmodium* B5-
594 specific $CD4^+$ T cell subsets were identified with gating strategy as schematically depicted in **S7**
595 **Fig**. For follicular T cell staining with CXCR5, cells were stained in PBS + 0.5% BSA + 0.1%
596 sodium azide + 2% Normal Mouse Serum (NMS) and 2% FBS (Sigma, St. Louis, MO). Rat anti-
597 mouse purified CXCR5 (2G8, BDbioscience, San Jose, CA, 1 hr., 4°C) was followed by biotin-
598 conjugated AffiniPure Goat anti-rat (H+L, Jackson ImmunoResearch, West Grove, PA, 30 min,
599 4°C) followed by Streptavidin-eFluor 450. For antigen presenting cells were stained with anti-
600 Ly6C, anti-Ly6G (1A8), anti CD11b (M1/70), anti-CD11c (N418), DX5, MHCII/I-A/Eb
601 (M5/114.15.2). For intracellular cytokine staining, cells were cultured for 5 hours at 37°C, 5%
602 CO_2 in the presence of GolgiPlug (BD Bioscience) before extracellular staining and then fixed
603 with 2% paraformaldehyde overnight. Cells were then permeabilized using BD 10X Permeability
604 buffer diluted with water, and stained with anti-IFN-γ (XMG1.2), anti-TNF (MP6-XT22), anti-IL-
605 2 (JES6-5H4). Virus-specific $CD4^+$ T cells were identified using m78/I-A^d tetramers, with peptide
606 (SQQKMTSLPMSVFYS) and CLIP/I-A^d as tetramer control (PVSKMRMATPLLMQA) and
607 $CD8^+$ T cells with $H2D^d$ restricted m45-tetramer peptide 507-VGPALGRGL-515 [20, 21] (both
608 from NIH Tetramer Core Facility, Emory, Atlanta, GA). Tetramer staining was performed within
609 6 months of receiving the reagents at 4C for 1 hour before/after surface and intracellular staining.
610 Cells were acquired on a LSR II Fortessa using FACSDiva software (BD Biosciences, San Jose,
611 CA). Compensation was performed in FlowJo using single-stained splenocytes (with CD4 in all
612 colors). All data analysis was performed using the FlowJo software package (version 10, FlowJo,
613 BD San Jose, CA). Cell numbers were calculated as the % of recovered Tg cells/lymphocytes x
614 the number of lymphocytes, except for **Fig 6** and **Fig 7** which the recovered cells were counted by

615 inclusion of counting beads (Accu-Check, Molecular Probes, Thermo Fisher Scientific) in the
616 FACS sample according to manufacturer's instructions and calculated using the equation: Total
617 cell number = ((all cell event count / bead event count) x bead conc. (per µl) x (bead volume / cell
618 volume)) x volume of original sample. This formula only works if the whole volume of FACS
619 tube is collected.
620
621 **Cytokines and antibody measurements**
622 Cytokines and chemokines (CXCL10 (IP-10), IFN-γ, IFN-β, IFN-α, IL-10, IL-12p40, IL-
623 15, IL-18, IL-6, and TNF-α) were measured in the plasma by Legendplex according to
624 manufacturer's protocol (Biolegend, San Diego, CA). Plasma samples were collected at the
625 indicated days and were stored in -80°C until analysis. All data were acquired on an LSR II
626 Fortessa flow cytometer using FACSDiva software, version 8 (BD Biosciences, San Jose, CA).
627 The concentration of each analyte is determined with cytometric data based on a standard curve
628 using the LEGENDplex™ data analysis software (Biolegend, San Diego, CA). *P. chabaudi* AJ-
629 specific IgG was evaluated in plasma at indicated days by ELISA, as described previously [5].
630 Plates were coated with *P. chabaudi* AJ parasite lysate overnight at 4°C in PBS with 0.05%
631 Sodium Azide. Plates were blocked with 1% BSA, 0.3% Tween 20, 0.05% Sodium Azide and then
632 sera were incubated. Bound antibody was detected using Alkaline Phosphatase-conjugated goat
633 anti-mouse IgG (Southern Biotech, Birmingham, AL). The reaction was revealed with a p-
634 Nitrophenyl phosphate disodium salt (Sigma, USA) solution (1mg/ml) in diethanolamine buffer.
635 Plates were analyzed with an Omega plate reader (FLUOstar Omega BMG LABTECH Inc,
636 Durham, NC, USA).
637

638 **Statistical analysis**

639 All data were analyzed by ANOVA, followed by Tukey's or two-tailed Mann-Whitney test
640 or two-tailed unpaired Student t test, where indicated. All data are presented as mean ± SEM.
641 Statistical tests were performed using the statistical software package in Prism (version 9.2,
642 GraphPad Software, USA): *$p < 0.05$, **$p \leq 0.01$, ***$p \leq 0.001$ and n.s., not significant.

643

644 **Supporting information**

645

646 **Acknowledgments**

647 We would like to thank Florentin Aussenac, Victor H. Carpio, Nadia D. Domingo, Lucinda Puebla-
648 Clark and Peter Fleming for feedback and discussion. Thanks to Maria I. Giraldo Giraldo and
649 Gregg Milligan for technical advice. We thank the NIH Tetramer Core Facility at Emory, Atlanta,
650 GA for generating both the m78-Tetramer and m-45-Tetramer used in this study. This work was
651 supported by the James W. McLaughlin Fellowship Fund (KG) and NIH R01AI135061,
652 R01AI089953 (RS, KG).

653 **Author Contributions**

654 **Conceptualization:** KG, MGB, MAD, RS

655 **Investigation:** KG, SAI

656 **Formal Analysis:** KG, SAI, RS

657 **Methodology and Resources:** KG, SAI, MLO, MAD, MGB

658 **Funding acquisition:** KG, RS, MGB, MAD

659 **Project Administration, Supervision:** RS, MAD

660 **Writing – Original Draft Preparation:** KG

Writing – Review & Editing: RS, MGB, MAD

663 **References**

664 1. Kennedy RB, Ovsyannikova IG, Palese P, Poland GA. Current Challenges in Vaccinology.
665 Front Immunol. 2020;11:1181. Epub 2020/07/17. doi: 10.3389/fimmu.2020.01181. PubMed
666 PMID: 32670279; PubMed Central PMCID: PMCPMC7329983.

667 2. Pollard AJ, Bijker EM. A guide to vaccinology: from basic principles to new
668 developments. Nat Rev Immunol. 2021;21(2):83-100. Epub 2020/12/24. doi: 10.1038/s41577-
669 020-00479-7. PubMed PMID: 33353987; PubMed Central PMCID: PMCPMC7754704.

670 3. Freitas do Rosario AP, Muxel SM, Rodriguez-Malaga SM, Sardinha LR, Zago CA,
671 Castillo-Mendez SI, et al. Gradual decline in malaria-specific memory T cell responses leads to
672 failure to maintain long-term protective immunity to *Plasmodium chabaudi* AS despite persistence
673 of B cell memory and circulating antibody. J Immunol. 2008;181(12):8344-55. PubMed PMID:
674 19050251.

675 4. Palacpac NMQ, Horii T. Malaria vaccines: facing unknowns. F1000Res. 2020;9. Epub
676 2020/05/14. doi: 10.12688/f1000research.22143.1. PubMed PMID: 32399189; PubMed Central
677 PMCID: PMCPMC7194457.

678 5. Achtman AH, Stephens R, Cadman ET, Harrison V, Langhorne J. Malaria-specific
679 antibody responses and parasite persistence after infection of mice with *Plasmodium chabaudi*
680 chabaudi. Parasite Immunol. 2007;29(9):435-44. doi: 10.1111/j.1365-3024.2007.00960.x.
681 PubMed PMID: 17727567.

682 6. Scott P, Artis D, Uzonna J, Zaph C. The development of effector and memory T cells in
683 cutaneous leishmaniasis: the implications for vaccine development. Immunol Rev. 2004;201:318-
684 38. Epub 2004/09/14. doi: 10.1111/j.0105-2896.2004.00198.x. PubMed PMID: 15361250.

685 7. Peters NC, Pagan AJ, Lawyer PG, Hand TW, Henrique Roma E, Stamper LW, et al.
686 Chronic parasitic infection maintains high frequencies of short-lived Ly6C+CD4+ effector T cells
687 that are required for protection against re-infection. PLoS Pathog. 2014;10(12):e1004538. Epub
688 2014/12/05. doi: 10.1371/journal.ppat.1004538. PubMed PMID: 25473946; PubMed Central
689 PMCID: PMCPMC4256462.
690 8. Stephens R, Langhorne J. Effector memory Th1 CD4 T cells are maintained in a mouse
691 model of chronic malaria. PLoS Pathog. 2010;6(11):e1001208. Epub 2010/12/03. doi:
692 10.1371/journal.ppat.1001208. PubMed PMID: 21124875; PubMed Central PMCID:
693 PMCPMC2991260.
694 9. Zaph C, Uzonna J, Beverley SM, Scott P. Central memory T cells mediate long-term
695 immunity to Leishmania major in the absence of persistent parasites. Nat Med. 2004;10(10):1104-
696 10. Epub 2004/09/28. doi: 10.1038/nm1108. PubMed PMID: 15448686.
697 10. Opata MM, Ibitokou SA, Carpio VH, Marshall KM, Dillon BE, Carl JC, et al. Protection
698 by and maintenance of CD4 effector memory and effector T cell subsets in persistent malaria
699 infection. PLoS Pathog. 2018;14(4):e1006960. doi: 10.1371/journal.ppat.1006960. PubMed
700 PMID: 29630679; PubMed Central PMCID: PMCPMC5908200.
701 11. Stephens R, Albano FR, Quin S, Pascal BJ, Harrison V, Stockinger B, et al. Malaria-
702 specific transgenic CD4(+) T cells protect immunodeficient mice from lethal infection and
703 demonstrate requirement for a protective threshold of antibody production for parasite clearance.
704 Blood. 2005;106(5):1676-84. doi: 10.1182/blood-2004-10-4047. PubMed PMID: 15890689.
705 12. Ibitokou SA, Gbedande K, Opata MM, Carpio VH, Marshall KM, Stephens R. Effects of
706 Low-Level Persistent Infection on Maintenance of Immunity by CD4 T Cell Subsets and Th1

707 Cytokines. Infect Immun. 2023;91(3):e0053122. Epub 2023/03/16. doi: 10.1128/iai.00531-22.
708 PubMed PMID: 36920200; PubMed Central PMCID: PMCPMC10016079.
709 13. Hansen SG, Vieville C, Whizin N, Coyne-Johnson L, Siess DC, Drummond DD, et al.
710 Effector memory T cell responses are associated with protection of rhesus monkeys from mucosal
711 simian immunodeficiency virus challenge. Nat Med. 2009;15(3):293-9. Epub 2009/02/17. doi:
712 10.1038/nm.1935. PubMed PMID: 19219024; PubMed Central PMCID: PMC2720091.
713 14. Beverley PC, Ruzsics Z, Hey A, Hutchings C, Boos S, Bolinger B, et al. A novel murine
714 cytomegalovirus vaccine vector protects against Mycobacterium tuberculosis. J Immunol.
715 2014;193(5):2306-16. doi: 10.4049/jimmunol.1302523. PubMed PMID: 25070842; PubMed
716 Central PMCID: PMCPMC4134927.
717 15. Hansen SG, Ford JC, Lewis MS, Ventura AB, Hughes CM, Coyne-Johnson L, et al.
718 Profound early control of highly pathogenic SIV by an effector memory T-cell vaccine. Nature.
719 2011;473(7348):523-7. doi: 10.1038/nature10003. PubMed PMID: 21562493; PubMed Central
720 PMCID: PMCPMC3102768.
721 16. Hansen SG, Womack J, Scholz I, Renner A, Edgel KA, Xu G, et al. Cytomegalovirus
722 vectors expressing *Plasmodium knowlesi* antigens induce immune responses that delay parasitemia
723 upon sporozoite challenge. PLoS One. 2019;14(1):e0210252. doi: 10.1371/journal.pone.0210252.
724 PubMed PMID: 30673723; PubMed Central PMCID: PMCPMC6343944 VIR Biotechnology
725 Inc., a company that may have a commercial interest in the results of this research and technology.
726 The potential individual and institutional conflicts of interest have been reviewed and managed by
727 OHSU. This does not alter our adherence to PLOS ONE policies on sharing data and materials.
728 17. Tsuda Y, Parkins CJ, Caposio P, Feldmann F, Botto S, Ball S, et al. A cytomegalovirus-
729 based vaccine provides long-lasting protection against lethal Ebola virus challenge after a single

730 dose. Vaccine. 2015;33(19):2261-6. Epub 2015/03/31. doi: 10.1016/j.vaccine.2015.03.029.
731 PubMed PMID: 25820063; PubMed Central PMCID: PMCPMC4402448.
732 18. Wilski NA, Snyder CM. From Vaccine Vector to Oncomodulation: Understanding the
733 Complex Interplay between CMV and Cancer. Vaccines (Basel). 2019;7(3). Epub 2019/07/22. doi:
734 10.3390/vaccines7030062. PubMed PMID: 31323930; PubMed Central PMCID:
735 PMCPMC6789822.
736 19. Snyder CM, Cho KS, Bonnett EL, Allan JE, Hill AB. Sustained CD8+ T cell memory
737 inflation after infection with a single-cycle cytomegalovirus. PLoS Pathog. 2011;7(10):e1002295.
738 doi: 10.1371/journal.ppat.1002295. PubMed PMID: 21998590; PubMed Central PMCID:
739 PMCPMC3188546.
740 20. Snyder CM, Cho KS, Bonnett EL, van Dommelen S, Shellam GR, Hill AB. Memory
741 inflation during chronic viral infection is maintained by continuous production of short-lived,
742 functional T cells. Immunity. 2008;29(4):650-9. doi: 10.1016/j.immuni.2008.07.017. PubMed
743 PMID: 18957267; PubMed Central PMCID: PMCPMC2583440.
744 21. Verma S, Weiskopf D, Gupta A, McDonald B, Peters B, Sette A, et al. Cytomegalovirus-
745 Specific CD4 T Cells Are Cytolytic and Mediate Vaccine Protection. J Virol. 2016;90(2):650-8.
746 Epub 2015/10/23. doi: 10.1128/JVI.02123-15. PubMed PMID: 26491148; PubMed Central
747 PMCID: PMCPMC4702662.
748 22. Barton ES, White DW, Cathelyn JS, Brett-McClellan KA, Engle M, Diamond MS, et al.
749 Herpesvirus latency confers symbiotic protection from bacterial infection. Nature.
750 2007;447(7142):326-9. Epub 2007/05/18. doi: 10.1038/nature05762. PubMed PMID: 17507983.
751 23. Furman D, Jojic V, Sharma S, Shen-Orr SS, Angel CJ, Onengut-Gumuscu S, et al.
752 Cytomegalovirus infection enhances the immune response to influenza. Sci Transl Med.

753 2015;7(281):281ra43. Epub 2015/04/04. doi: 10.1126/scitranslmed.aaa2293. PubMed PMID:
754 25834109; PubMed Central PMCID: PMCPMC4505610.
755 24. Andrews DM, Estcourt MJ, Andoniou CE, Wikstrom ME, Khong A, Voigt V, et al. Innate
756 immunity defines the capacity of antiviral T cells to limit persistent infection. J Exp Med.
757 2010;207(6):1333-43. Epub 2010/06/02. doi: 10.1084/jem.20091193. PubMed PMID: 20513749;
758 PubMed Central PMCID: PMCPMC2882831.
759 25. Campo JJ, Sacarlal J, Aponte JJ, Aide P, Nhabomba AJ, Dobano C, et al. Duration of
760 vaccine efficacy against malaria: 5th year of follow-up in children vaccinated with RTS,S/AS02
761 in Mozambique. Vaccine. 2014;32(19):2209-16. Epub 2014/03/19. doi:
762 10.1016/j.vaccine.2014.02.042. PubMed PMID: 24631081.
763 26. Raja AI, Cai Y, Reiman JM, Groves P, Chakravarty S, McPhun V, et al. Chemically
764 Attenuated Blood-Stage *Plasmodium yoelii* Parasites Induce Long-Lived and Strain-Transcending
765 Protection. Infect Immun. 2016;84(8):2274-88. Epub 2016/06/02. doi: 10.1128/IAI.00157-16.
766 PubMed PMID: 27245410; PubMed Central PMCID: PMC4962623.
767 27. Pombo DJ, Lawrence G, Hirunpetcharat C, Rzepczyk C, Bryden M, Cloonan N, et al.
768 Immunity to malaria after administration of ultra-low doses of red cells infected with *Plasmodium*
769 *falciparum*. Lancet. 2002;360(9333):610-7. Epub 2002/09/21. doi: 10.1016/S0140-
770 6736(02)09784-2. PubMed PMID: 12241933.
771 28. Holtappels R, Pahl-Seibert MF, Thomas D, Reddehase MJ. Enrichment of immediate-early
772 1 (m123/pp89) peptide-specific CD8 T cells in a pulmonary CD62L(lo) memory-effector cell pool
773 during latent murine cytomegalovirus infection of the lungs. J Virol. 2000;74(24):11495-503.
774 Epub 2000/11/23. doi: 10.1128/jvi.74.24.11495-11503.2000. PubMed PMID: 11090146; PubMed
775 Central PMCID: PMCPMC112429.

776 29. Farrand KJ, Dickgreber N, Stoitzner P, Ronchese F, Petersen TR, Hermans IF. Langerin+
777 CD8alpha+ dendritic cells are critical for cross-priming and IL-12 production in response to
778 systemic antigens. J Immunol. 2009;183(12):7732-42. Epub 2009/11/20. doi:
779 10.4049/jimmunol.0902707. PubMed PMID: 19923446.
780 30. RTS. Efficacy and safety of RTS,S/AS01 malaria vaccine with or without a booster dose
781 in infants and children in Africa: final results of a phase 3, individually randomised, controlled
782 trial. Lancet. 2015;386(9988):31-45. Epub 2015/04/29. doi: 10.1016/S0140-6736(15)60721-8.
783 PubMed PMID: 25913272; PubMed Central PMCID: PMC5626001.
784 31. Rts SCTP. Efficacy and safety of the RTS,S/AS01 malaria vaccine during 18 months after
785 vaccination: a phase 3 randomized, controlled trial in children and young infants at 11 African
786 sites. PLoS Med. 2014;11(7):e1001685. doi: 10.1371/journal.pmed.1001685. PubMed PMID:
787 25072396; PubMed Central PMCID: PMCPMC4114488.
788 32. Draper SJ, Sack BK, King CR, Nielsen CM, Rayner JC, Higgins MK, et al. Malaria
789 Vaccines: Recent Advances and New Horizons. Cell Host Microbe. 2018;24(1):43-56. Epub
790 2018/07/13. doi: 10.1016/j.chom.2018.06.008. PubMed PMID: 30001524; PubMed Central
791 PMCID: PMCPMC6054918.
792 33. Cicin-Sain L, Sylwester AW, Hagen SI, Siess DC, Currier N, Legasse AW, et al.
793 Cytomegalovirus-specific T cell immunity is maintained in immunosenescent rhesus macaques. J
794 Immunol. 2011;187(4):1722-32. doi: 10.4049/jimmunol.1100560. PubMed PMID: 21765018;
795 PubMed Central PMCID: PMCPMC3151292.
796 34. Snyder CM, Loewendorf A, Bonnett EL, Croft M, Benedict CA, Hill AB. CD4+ T cell
797 help has an epitope-dependent impact on CD8+ T cell memory inflation during murine
798 cytomegalovirus infection. J Immunol. 2009;183(6):3932-41. Epub 2009/08/21. doi:

799 10.4049/jimmunol.0900227. PubMed PMID: 19692644; PubMed Central PMCID:
800 PMCPMC2766182.
801 35. Meding SJ, Langhorne J. CD4+ T cells and B cells are necessary for the transfer of
802 protective immunity to *Plasmodium chabaudi chabaudi*. Eur J Immunol. 1991;21(6):1433-8. doi:
803 10.1002/eji.1830210616. PubMed PMID: 1675172.
804 36. Lemmermann NAW, Reddehase MJ. Direct Evidence for Viral Antigen Presentation
805 during Latent Cytomegalovirus Infection. Pathogens. 2021;10(6). Epub 2021/07/03. doi:
806 10.3390/pathogens10060731. PubMed PMID: 34200578; PubMed Central PMCID:
807 PMCPMC8229173.
808 37. Simon CO, Holtappels R, Tervo HM, Bohm V, Daubner T, Oehrlein-Karpi SA, et al. CD8
809 T cells control cytomegalovirus latency by epitope-specific sensing of transcriptional reactivation.
810 J Virol. 2006;80(21):10436-56. Epub 2006/08/25. doi: 10.1128/JVI.01248-06. PubMed PMID:
811 16928768; PubMed Central PMCID: PMCPMC1641801.
812 38. Mashayekhi M, Sandau MM, Dunay IR, Frickel EM, Khan A, Goldszmid RS, et al.
813 CD8alpha(+) dendritic cells are the critical source of interleukin-12 that controls acute infection
814 by *Toxoplasma gondii* tachyzoites. Immunity. 2011;35(2):249-59. Epub 2011/08/27. doi:
815 10.1016/j.immuni.2011.08.008. PubMed PMID: 21867928; PubMed Central PMCID:
816 PMCPMC3171793.
817 39. Garris CS, Arlauckas SP, Kohler RH, Trefny MP, Garren S, Piot C, et al. Successful Anti-
818 PD-1 Cancer Immunotherapy Requires T Cell-Dendritic Cell Crosstalk Involving the Cytokines
819 IFN-gamma and IL-12. Immunity. 2018;49(6):1148-61 e7. Epub 2018/12/16. doi:
820 10.1016/j.immuni.2018.09.024. PubMed PMID: 30552023; PubMed Central PMCID:
821 PMCPMC6301092.

822 40. Grohmann U, Belladonna ML, Vacca C, Bianchi R, Fallarino F, Orabona C, et al. Positive
823 regulatory role of IL-12 in macrophages and modulation by IFN-gamma. J Immunol.
824 2001;167(1):221-7. Epub 2001/06/22. doi: 10.4049/jimmunol.167.1.221. PubMed PMID:
825 11418652.
826 41. Su Z, Stevenson MM. IL-12 is required for antibody-mediated protective immunity against
827 blood-stage *Plasmodium chabaudi* AS malaria infection in mice. J Immunol. 2002;168(3):1348-
828 55. Epub 2002/01/22. doi: 10.4049/jimmunol.168.3.1348. PubMed PMID: 11801675.
829 42. Meding SJ, Cheng SC, Simon-Haarhaus B, Langhorne J. Role of gamma interferon during
830 infection with *Plasmodium chabaudi chabaudi*. Infect Immun. 1990;58(11):3671-8. Epub
831 1990/11/01. doi: 10.1128/iai.58.11.3671-3678.1990. PubMed PMID: 1977706; PubMed Central
832 PMCID: PMCPMC313713.
833 43. Chen ZM, Yang XY, Li ZT, Guan WJ, Qiu Y, Li SQ, et al. Anti-Interferon-gamma
834 Autoantibodies Impair T-Lymphocyte Responses in Patients with Talaromyces marneffei
835 Infections. Infect Drug Resist. 2022;15:3381-93. Epub 2022/07/06. doi: 10.2147/IDR.S364388.
836 PubMed PMID: 35789796; PubMed Central PMCID: PMCPMC9250332.
837 44. da Silva HB, de Salles EM, Panatieri RH, Boscardin SB, Rodriguez-Malaga SM, Alvarez
838 JM, et al. IFN-gamma-induced priming maintains long-term strain-transcending immunity against
839 blood-stage *Plasmodium chabaudi* malaria. J Immunol. 2013;191(10):5160-9. Epub 2013/10/18.
840 doi: 10.4049/jimmunol.1300462. PubMed PMID: 24133169.
841 45. Caposio P, van den Worm S, Crawford L, Perez W, Kreklywich C, Gilbride RM, et al.
842 Characterization of a live-attenuated HCMV-based vaccine platform. Sci Rep. 2019;9(1):19236.
843 Epub 2019/12/19. doi: 10.1038/s41598-019-55508-w. PubMed PMID: 31848362; PubMed
844 Central PMCID: PMCPMC6917771.

845 46. Liu J, Jaijyan DK, Tang Q, Zhu H. Promising Cytomegalovirus-Based Vaccine Vector
846 Induces Robust CD8(+) T-Cell Response. Int J Mol Sci. 2019;20(18). Epub 2019/09/13. doi:
847 10.3390/ijms20184457. PubMed PMID: 31510028; PubMed Central PMCID:
848 PMCPMC6770317.
849 47. Landau I, Killick-Kendrick R. Rodent plasmodia of the Republique Centrafricaine: the
850 sporogony and tissue stages of *Plasmodium chabaudi* and P. berghei yoelii. Trans R Soc Trop Med
851 Hyg. 1966;60(5):633-49. Epub 1966/01/01. doi: 10.1016/0035-9203(66)90010-1. PubMed PMID:
852 4163669.
853 48. Martinelli A, Hunt P, Fawcett R, Cravo PV, Walliker D, Carter R. An AFLP-based genetic
854 linkage map of *Plasmodium chabaudi chabaudi*. Malar J. 2005;4:11. Epub 2005/02/15. doi:
855 10.1186/1475-2875-4-11. PubMed PMID: 15707493; PubMed Central PMCID:
856 PMCPMC550669.
857 49. Corbett AJ, Coudert JD, Forbes CA, Scalzo AA. Functional consequences of natural
858 sequence variation of murine cytomegalovirus m157 for Ly49 receptor specificity and NK cell
859 activation. J Immunol. 2011;186(3):1713-22. Epub 2010/12/29. doi: 10.4049/jimmunol.1003308.
860 PubMed PMID: 21187440.
861 50. Wheat RL, Clark PY, Brown MG. Quantitative measurement of infectious murine
862 cytomegalovirus genomes in real-time PCR. J Virol Methods. 2003;112(1-2):107-13. PubMed
863 PMID: 12951218.
864
865

866 **Figure Legends**

867

868 **Figure 1. Prior MCMV infection protects against *P. chabaudi* infection.**

869 **(A)** Experimental schematic shows mice infected with MCMV-B5 or -BAC and challenged on
870 day 60 post MCMV infection with *P. chabaudi* AS. **(B)** Parasitemia and **(C)** weight loss were
871 determined after challenge. Data are representative of three independent experiments with 5
872 animals per group. Groups were compared using ANOVA followed by Tukey's post-test with
873 *, $P < 0.05$; **, $P < 0.01$. Mean shown with error bars representing SEM.

874

875 **Figure 2. MCMV-B5 stimulates and maintains parasite-specific effector T cell responses.**

876 **(A)** Experimental schematic shows MSP-1 specific B5 TCR Tg CD4 T cells ($CTV^{-}Thy1.2^{+}$) were
877 adoptively transferred into Thy1.1 mice that were then infected with MCMV-BAC or MCMV-B5.
878 Splenic T cells were gated on B5 TCR Tg ($CD4^{+}CTV^{-}Thy1.2^{+}$) recovered at days 15 and 55 post-
879 MCMV infection. **(B)** Plot, histogram and graphs show gating of proliferated B5 T cells. **(C)** Plots
880 and graphs show B5 Teff ($CD4^{+}Thy1.2^{+}CTV^{-}$, $CD127^{-}CD44^{hi}$) and Tmem ($CD4^{+}Thy1.2^{+}CTV^{-}$,
881 $CD127^{hi}CD44^{hi}$) **(D)** on day 15, or **(E)** day 55. Plots and graphs show B5 GC Tfh days 15 and 55
882 p.i.. Plots are concatenated from 3-5 animals per group. Data are representative of two experiments
883 with 3-5 mice in each group. Mean shown with error bars representing SEM and analyzed using
884 One-Way ANOVA followed by Tukey's post-test; *, $P < 0.05$; **, $P < 0.01$.

885

886 **Fig 3. MCMV boosts long-term protection of live malaria vaccine.**

887 **(A)** Experimental schematic shows infection and drug-cure live vaccine combined with MCMV
888 boosting strategy for protection to heterologous rechallenge. Mice were infected with *P. chabaudi*

889 AS and treated with two subsequent non-curative doses of chloroquine (CQ). Some groups
890 received MCMV-BAC or MCMV-B5 booster at day 140 (bottom timeline). All mice were
891 challenged with heterologous *P. chabaudi* AJ strain 200 days after live vaccination. Graph
892 showing **(B)** parasitemia of *P. chabaudi* AJ challengeand **(C)** serum level of *P. chabaudi* AJ-
893 specific IgG antibody at day 7 post-challenge. Data are representative of two independent
894 experiments with five mice per group showing mean, with error bars representing SEM and
895 analyzed using ANOVA followed by Tukey's post-test with **, $P < 0.01$; n.s., not significant.
896
897 **Fig 4. MCMV-B5 promotes maintenance of *Plasmodium*-specific effector T cells. (A)**
898 Experimental schematic shows live vaccine combined with MCMV boosting strategy with
899 adoptively transferred $CD4^+$ *Plasmodium* MSP1-specific T cells (B5 TCR Tg). $CD4^+$ $Thy1.2^+$
900 CTV^+ B5 T cells were adoptively transferred into Thy1.1 mice that were then vaccinated. Recipient
901 mice received MCMV-BAC or MCMV–B5 boosters at day 140, with T cell phenotyping at day
902 200 post-vaccination (p.v.). **(B)** Plot, histogram and graph show gating and quantification of
903 parasite-specific CTV^- B5 T cells recovered on d200. **(C)** Plots and graphs showing number of
904 Teff ($CD127^-$) and Tmem ($CD127^{hi}CD44^{hi}$) out of CTV^- B5 TCR Tg cells on day 200. **(D)** Plots
905 and graphs showing percentage and number of B5 memory T cell subsets gated on $CD44^{hi}CD127^{hi}$,
906 Tcm ($CD62L^+CD27^+$), Tem^{Early} (TemE, $CD62L^{lo}CD27^+$) or Tem^{Late} (TemL, $CD62L^{lo}CD27^-$).
907 Cytokines in B5 T cells were quantified and shown as histograms and graphs quantifying **(E)** IFN-
908 γ, **(F)** IL-2- and **(G)** TNF- positive CTV^- B5 T cells. Data are representative of two independent
909 experiments. Plots are concatenated from 5 animals per group, while graphs include individual
910 animals and show mean with error bars representing SEM. Groups were analyzed using One-Way
911 ANOVA followed by Tukey's post-test with *, $P < 0.05$; **, $P < 0.01$, ***, $P < 0.001$.

912

913 **Fig 5. IFN-γ induced by MCMV leads to increased cytokines and protection from *P. chabaudi***
914 **infection.**

915 **(A)** Experimental schematic shows mice infected with MCMV-BAC and anti-IFN-γ or isotype
916 control was administered at indicated days (34, 36 and 38 p.i.) prior to challenge with *P. chabaudi*
917 at day 40. Graphs show **(B)** percentage of parasitemia, **(C)** weight loss and **(D)** hypothermia upon
918 *P. chabaudi* challenge. **(E)** Plot and graph show fraction of polyclonal effector T cells at day 15
919 p.c., isotype in white and anti-IFN-γ in black bars. Graphs show plasma IL-12 p40 levels **(F)**
920 throughout MCMV infection and **(G)** after *P. chabaudi* challenge. **(H)** Graphs show chemokines
921 and cytokines on day 7 of *P. chabaudi* challenge after MCMV-BAC and antibody treatment.
922 Graphs include 5 animals per group and show mean with error bars representing SEM. Multiple
923 comparisons Student *t* test and Unpaired or Mann Whitney were used for all except (F) which was
924 analyzed with One-Way ANOVA. *, $P < 0.05$; **, $P < 0.01$, ***, $P < 0.001$; n.s., not significant.

925

926 **Fig 6: IFN-γ induced by MCMV does not regulate MCMV driven T cell phenotype, but does**
927 **induce IL-12 p40.**

928 **(A)** Experimental schematic shows CTV-labelled B5 TCR Tg T cells were adoptively transfer into
929 Thy1.1 (Balb/c) mice which were then infected with MCMV-B5 and received anti-IFN-γ antibody
930 or isotype at indicated time points and spleen phenotyped for dendritic cells and B5 TCR Tg
931 (Thy1.2$^+$) CD4$^+$ T cell at day 50 p.i.. **(B)** Plot, histogram and graph show gating and quantification
932 of CD4$^+$Thy1.2$^+$CTV$^-$ B5 T cells. **(C)** Plots and summary bar graph show MCMV-B5-specific
933 effector and memory T cell numbers. **(D)** Plot and summary bar graph show the number within
934 each MCMV-B5-specific Tmem subset (Tcm, TemE and TemL) as defined by CD27 and CD62L

935 **(E)** Plot and histogram show DC and CD8α DC population gating and quantification forCD8α$^-$
936 DC, CD8α$^+$ DC and **(F)** serum IL-12p40 levels. Data shown are representative 5 mice per group
937 and mean shown with error bars representing SEM. The Student *t* test was used; *, $P < 0.05$.
938
939 **Fig 7. IFN-γ induced by MCMV vector drives increase in CD8α$^+$ dendritic cells, and boost of**
940 **long-term protection by live malaria vaccine.**
941 **(A)** Experimental schematic shows B5 TCR Tg CD4 T cells labelled with cell trace violet (CTV)
942 were adoptively transferred into Thy1.1 mice that were then vaccinated with live malaria vaccine.
943 Recipient vaccinated mice received MCMV-B5 boosters at day 140 and then received anti-IFN-γ
944 antibody or isotype at indicated days (194, 196, 198) before spleen cell recovery for phenotyping
945 at day 200 p.v. **(B)** Plot, histogram and graph show gating and quantification of B5-epitope-
946 specific T cells (CTV$^-$Thy1.2$^+$) recovered on day 200. **(C)** Plot and summary bar graph show the
947 number within each vaccine and booster-B5-specific Tmem subset (Tcm, TemE and TemL) as
948 defined by CD27 and CD62L. * indicates significant difference between TemL subsets recovered
949 between groups. **(D)** Plots and graphs show gating and number of total DC population (CD3$^-$
950 CD11c^{hi}MHCII^{hi}), and **(E)** CD8α$^-$ or CD8α$^+$ DC. Plots are concatenated from 5 animals per group.
951 **(F)** Graph of serum IL-12p40 level at day 200 p.v. before and after boosting. **(G)** Experimental
952 schematic for infection and drug-cure vaccine combined with MCMV boosting strategy for
953 protection to heterologous rechallenge. Age-matched mice were infected with *P. chabaudi* AS and
954 treated with two subsequent non-curative doses of chloroquine (CQ). Then they received MCMV
955 booster at day 140. Some mice received anti-IFN-γ antibody or isotype at indicated days (194,
956 196, 198) after *P. chabaudi* vaccination. All mice were reinfected with *P. chabaudi* AJ strain at
957 200 days p.v. Graphs showing **(H)** weight loss and **(I)** parasitemia after *P. chabaudi* AJ challenge

958 or infection. Comparisons of vaccinated or non-vaccinated groups are significantly different by
959 ANOVA and Tukey's multiple comparisons significance is not shown for the sake of simplicity
960 ($p < 0.01$, for all time points for parasitemia and at day 9 p.c. for weight loss). **(J)** Graphs showing
961 parasitemia on day 5 *P. chabaudi* AJ challenge after IFN-γ neutralization (black bar) compared to
962 isotype (grey bar). **(K)** Graph of fraction of polyclonal effector T cells ($CD127^-$) responding to
963 challenge (d15 p.c.). **(L) graph of** serum level of *P. chabaudi* AJ-specific IgG antibody at
964 indicated days (-5, 7 and 15) relative to challenge. Data shown represent 5 animals per group.
965 Mean shown with error bars representing SEM. Groups were analyzed using ANOVA followed
966 by Tukey's post-test for all except (J and K) which were analyzed with Student *t* test. *, $P < 0.05$;
967 **, $P < 0.01$, ***, $P < 0.001$; n.s., not significant.
968
969 **S1 Fig. *Plasmodium chabaudi* MSP-1 B5 antigen-expressing MCMV vaccine vector**.
970 **(A)** *P. chabaudi* merozoite surface protein MSP-1 (B5:1157–1171) B5 epitope is expressed as an
971 MCMV immediate early gene. B5 epitope was introduced into an MCMV-K181 bacterial artificial
972 chromosome (BAC) using recombineering. **(B)** The indicated organs were collected from MCMV
973 infected mice at different times post- MCMV infection, homogenized, and MCMV titres were
974 determined by plaque assay. The dashed line represents the limit of detection (L.O.D.) for each
975 organ. Mean ± SEM are plotted with three mice for each time point. **(C)** Time course of qPCR
976 assessment of MCMV infection in multiple organs. Mice were infected with MCMV-B5 or
977 MCMV-BAC and organs were collected at indicated times for vector quantification with n=6 per
978 time point. Copy number of CMV/β-actin (±SEM) ratio and L.O.D. of the assay are shown. L.O.D
979 was calculated using data from uninfected animal. (**D**) Mice were infected with MCMV-BAC or
980 MCMV-B5 and splenocytes were recovered 15 days later for MCMV-induced polyclonal T cell
981 phenotype. Plots show gating and graphs show numbers of polyclonal $CD4^+$ T cells effector

982 (CD127^{-}) and memory (CD44^{hi}CD127^{hi}) phenotype cells recovered after MCMV-B5 compared to
983 MCMV-BAC. **(E)** Enumeration of MCMV-specific m78-Tetramer-positive CD4 T cells upon
984 MCMV-B5 compared to MCMV-BAC from day 15 MCMV-infected mice. Plots represents
985 control CLIP tetramer or m-78-tetramer staining after MCMV-B5. Graph shows number of
986 MCMV-specific m78 Tet+ T cells (±SEM). **(F)** Enumeration of MCMV-specific m45-Tetramer-
987 positive CD8 T cells. Mice were infected with MCMV-B5 and splenocytes were recovered 11 and
988 60 days later for CD8 T cell quantification by staining with m45 tetramers. Plots and graph show
989 m45-Tet^{+} CD8^{+} T cells from uninfected and MCMV-B5 infected mice gating on vector specific T
990 cells (+/- SEM). Data shown are representative of two experiments with 3 or 5 mice each. Groups
991 were analyzed using One-Way ANOVA followed by Tukey's post-test with *, $P < 0.05$;
992 **, $P < 0.01$.
993
994 **S2 Fig. Persistent MCMV-B5 infection induces vector-specific T cell response and may**
995 **promote continued B5 TCR Tg T cell proliferation.**
996 **(A)** Experimental schematic shows mice were infected with MCMV-B5, and splenocytes were
997 recovered 11 or 60 days later to quantify MCMV m-78-specific Tetramer^{+} CD4 T cells. (**B**) Plots
998 and graph show uninfected and m78 tetramer-specific T cell numbers. Virus-specific CD4^{+} T cells
999 were identified using m78/I-A^{d} tetramers, with peptide (SQQKMTSLPMSVFYS) and CLIP/I-A^{d}
1000 as tetramer control (PVSKMRMATPLLMQA). (**C**) Plots and graphs show the number of MCMV-
1001 specific-Teff (CD44^{+}CD127^{-}) and Tmem (CD44^{hi}CD127^{hi}) in the spleen gated on MCMV m78-
1002 tetramer CD4^{+} T cell at day 11 and 60 p.i.. Data shown are representative of two experiments with
1003 5 mice each and error bars representing SEM. **(D)** Experimental Schematic shows MCMV-BAC
1004 or MCMV-B5 infection of different groups of age-matched Thy1.1 mice at indicated times (0, 30

1005 and 50 days) followed by adoptive transfer of CTV$^+$ B5 TCR Tg CD4 T cells to all groups 5 days
1006 before phenotyping, and 55 days after first infection. **(E)** Plots and graphs showing gating and
1007 frequency of CTV-B5 T cells out of CD4 T cells, or number of proliferated B5 epitope-specific
1008 CD4 T cells in response to MCMV-BAC or MCMV-B5 infection at different time points. Data are
1009 representative of three independent experiments with 5 animals per group. Mean shown with error
1010 bars representing SEM. Groups were analyzed using One-Way ANOVA followed by Tukey's
1011 post-test with *, $P < 0.05$; **, $P < 0.01$; ***, $P < 0.001$.
1012
1013 **S3 Fig. Decay of *P. chabaudi* protection by days 200**
1014 **(A)** Experimental schematic shows age-matched mice were infected with *P. chabaudi* AS for
1015 assessment of protection to heterologous challenge with *P. chabaudi* AJ 60 or 200 days later.
1016 Graphs show **(B)** the percentage of parasitemia (iRBC/RBC) after heterologous challenge, and **(C)**
1017 *P. chabaudi* AJ-specific IgG antibody serum level at day 7 post-challenge. Data are representative
1018 of two independent experiments with five mice per group showing mean, with error bars
1019 representing SEM. Groups were analyzed using One-Way ANOVA followed by Tukey's post-test
1020 with *, $P < 0.05$; **, $P < 0.01$; ***, $P < 0.001$.
1021
1022 **S4 Fig: Evaluation of neutralizing effect of anti-IFN-γ antibody**
1023 **(A)** Experimental schematic shows mice were infected or not infected with MCMV-BAC to assess
1024 the neutralizing effect of anti-IFN-γ naïve mice or in MCMV-induced protection to *P. chabaudi*.
1025 Blocking of IFN-γ *in vivo* with anti-IFN-γ antibody or isotype control antibody was performed at
1026 days 34, 36 and 38 prior to the challenge or infection with *P. chabaudi* at day 40 in both MCMV
1027 infected and naïve mice. Graphs show percentage of parasitemia in **(B)** no MCMV mice and **(C)**

1028 MCMV vaccinated mice**.** Relative CXCL-10 mRNA level normalized with β-actin from Raw
1029 264.7 cells cultured for 24h with sera from: (**D**) 2 days after anti-IFN-γ administration, (**E**) day 7
1030 post *P. chabaudi* challenge, (**F**) 2 days after anti-IFN-γ administration in presence of rIFN-γ
1031 (25ng/ml), and (**G**) day 7 post *P. chabaudi* challenge administration in presence of rIFN-γ
1032 (25ng/ml). Data shown represent 5 animals per group and mean shown with error bars representing
1033 SEM. Groups were analyzed using Student *t* test (C, D and F) or One-Way ANOVA (B, E and G)
1034 with *, $P < 0.05$; **, $P < 0.01$; ***, $P < 0.001$.
1035
1036 **S5 Fig. Combined IL-12 and IL-18 neutralization did not affect protection induced by**
1037 **MCMV.**
1038 **(A)** Experimental schematic shows mice infected with MCMV-BAC and the combination of anti-
1039 IL-12p40 and anti-IL-18 antibody or isotypes were given post MCMV infection. Graphs show
1040 percentage of parasitemia **(B)**, weight loss **(C)**, and hypothermia **(D)** upon combined IL-12 and
1041 IL-18 neutralization. Data shown represent 5 animals per group and mean shown with error bars
1042 representing SEM and analyzed using multiple comparisons Student *t* test; n.s., not significant.
1043
1044 **S6 Fig. IFN-γ induced by MCMV vector does not change most antigen-presenting cells types**
1045 **and their activation significantly.**
1046 **(A)** Experimental schematic shows mice infected with MCMV-B5 and received anti-IFN-γ
1047 antibody or isotype at indicated time points. Splenic antigen-presenting cells types (monocytes,
1048 macrophages and inflammatory monocytes) and NK cells were phenotyped at day 50 p.i.. **(B)**
1049 Plots and graphs show gating and quantification of $CD3^{-}CD11b^{-}Ly6C^{+}$, $CD3^{-}$ $CD11b^{+}Ly6C^{+}$,
1050 $CD3^{-}$ $CD11b^{+}Ly6C^{-}$ cells. (C) Histograms and graphs show MFI of CD3- CD11b+Ly6C-

1051 expressing activation marker MHCII. (D) Histograms and graphs show MFI of CD3-
1052 CD11b+Ly6C- expressing activation marker CD86. (**E**) Plots and graphs show gating and
1053 quantification of $CD3^-$ $DX5^+MHCII^-$ NK cells.
1054 (**F**) Experimental schematic shows Thy1.1 mice vaccinated with live malaria vaccine. Then
1055 vaccinated mice received MCMV-B5 boosters at day 140 and then received anti-IFN-γ antibody
1056 or isotype at indicated days (194, 196, 198) before spleen cell recovery for cells phenotyping at
1057 day 200 p.v. **(G)** Plots and graphs show gating and quantification of $CD3^-$ $CD11b^-Ly6C^+$, $CD3^-$
1058 $CD11b^+Ly6C^+$, $CD3^-$ $CD11b^+Ly6C^-$ cells. **(H)** Histograms and graphs show MFI of macrophages
1059 ($CD3^-CD11b^+Ly6C^-$) expressing activation marker MHCII. **(I)** Histograms and graphs show MFI
1060 of inflammatory monocytes ($CD3^-$ $CD11b^+Ly6C^+$) expressing activation marker MHCII. (**J**) Plots
1061 and graphs show gating and quantification of $CD3^-DX5^+MHCII^-$ NK cells. Data shown are
1062 representative 5 mice per group. Plots concatenated per group and mean shown with error bars
1063 representing SEM. The Student *t* test or One-Way ANOVA were used.
1064
1065 **S7 Fig. An example of a gating strategy used to identify polyclonal $CD4^+$ T cells subsets and**
1066 **B5-specific $CD4^+$ T cells subsets**
1067 **(Top row)** Plots show gating strategy for polyclonal $CD4^+$ T cell subsets Teff ($CD4^+CD127^-$
1068 $CD44^{hi}$), Tmem ($CD4^+CD127^{hi}CD44^{hi}$); and memory T cell subsets gated on $CD44^{hi}CD127^{hi}$ as
1069 Tcm ($CD62L^+CD27^+$), Tem^{Early} (TemE, $CD62L^{lo}CD27^+$) or Tem^{Late} (TemL, $CD62L^{lo}CD27^-$).
1070 **(Bottom row)** Plots show gating strategy for B5-specific T cells: Teff ($CD4^+Thy1.2^+CTV^-$,
1071 $CD127^-CD44^{hi}$), Tmem ($CD4^+Thy1.2^+CTV^-$, $CD127^{hi}CD44^{hi}$) and B5 memory T cell subsets
1072 gated on $CD44^{hi}CD127^{hi}$, Tcm ($CD62L^+CD27^+$), Tem^{Early} (TemE, $CD62L^{lo}CD27^+$) or Tem^{Late}
1073 (TemL, $CD62L^{lo}CD27^-$).

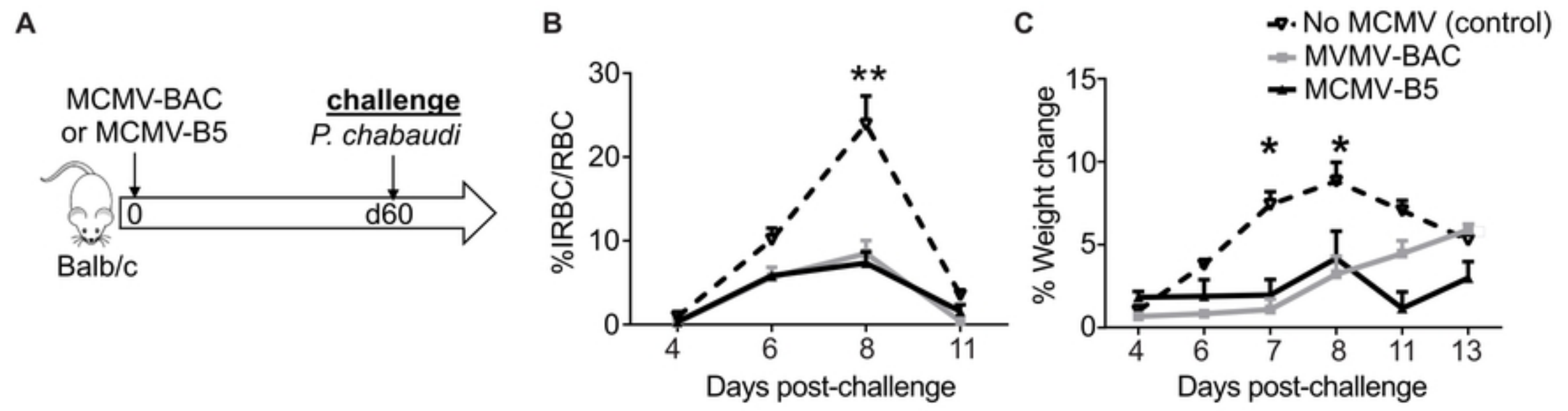
A
MCMV-BAC
or MCMV-B5
challenge
P. chabaudi
0
d60
Balb/c
B
%IRBC/RBC
30
20
10
0
**
4
6
8
11
Days post-challenge
C
No MCMV (control)
MVMV-BAC
MCMV-B5
% Weight change
15
10
5
0
*
*
4
6
7
8
11
13
Days post-challenge

Figure 1

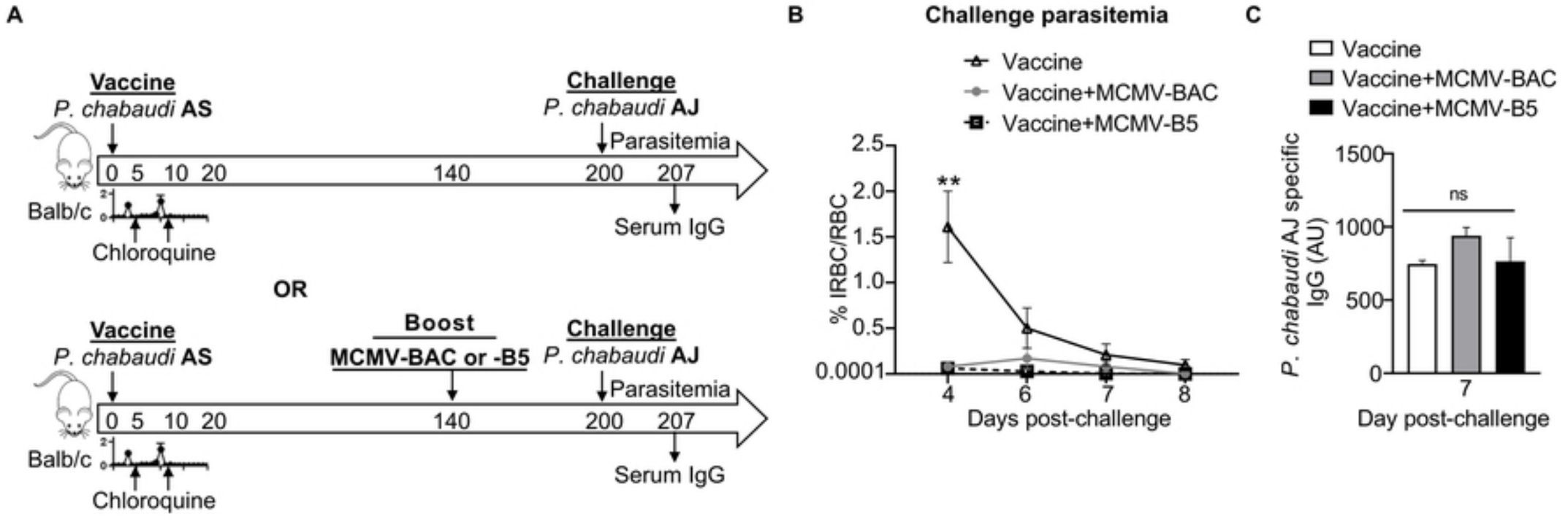
A
Vaccine
P. chabaudi AS
Challenge
P. chabaudi AJ
Parasitemia
0 5 10 20 140 200 207
Balb/c
Chloroquine
Serum IgG
OR
Vaccine
P. chabaudi AS
Boost
MCMV-BAC or -B5
Challenge
P. chabaudi AJ
Parasitemia
0 5 10 20 140 200 207
Balb/c
Chloroquine
Serum IgG
B
Challenge parasitemia
Vaccine
Vaccine+MCMV-BAC
Vaccine+MCMV-B5
% IRBC/RBC
2.5
2.0
1.5
1.0
0.5
0.0001
**
4 6 7 8
Days post-challenge
C
Vaccine
Vaccine+MCMV-BAC
Vaccine+MCMV-B5
P. chabaudi AJ specific IgG (AU)
1500
1000
500
0
ns
7
Day post-challenge

Figure 3

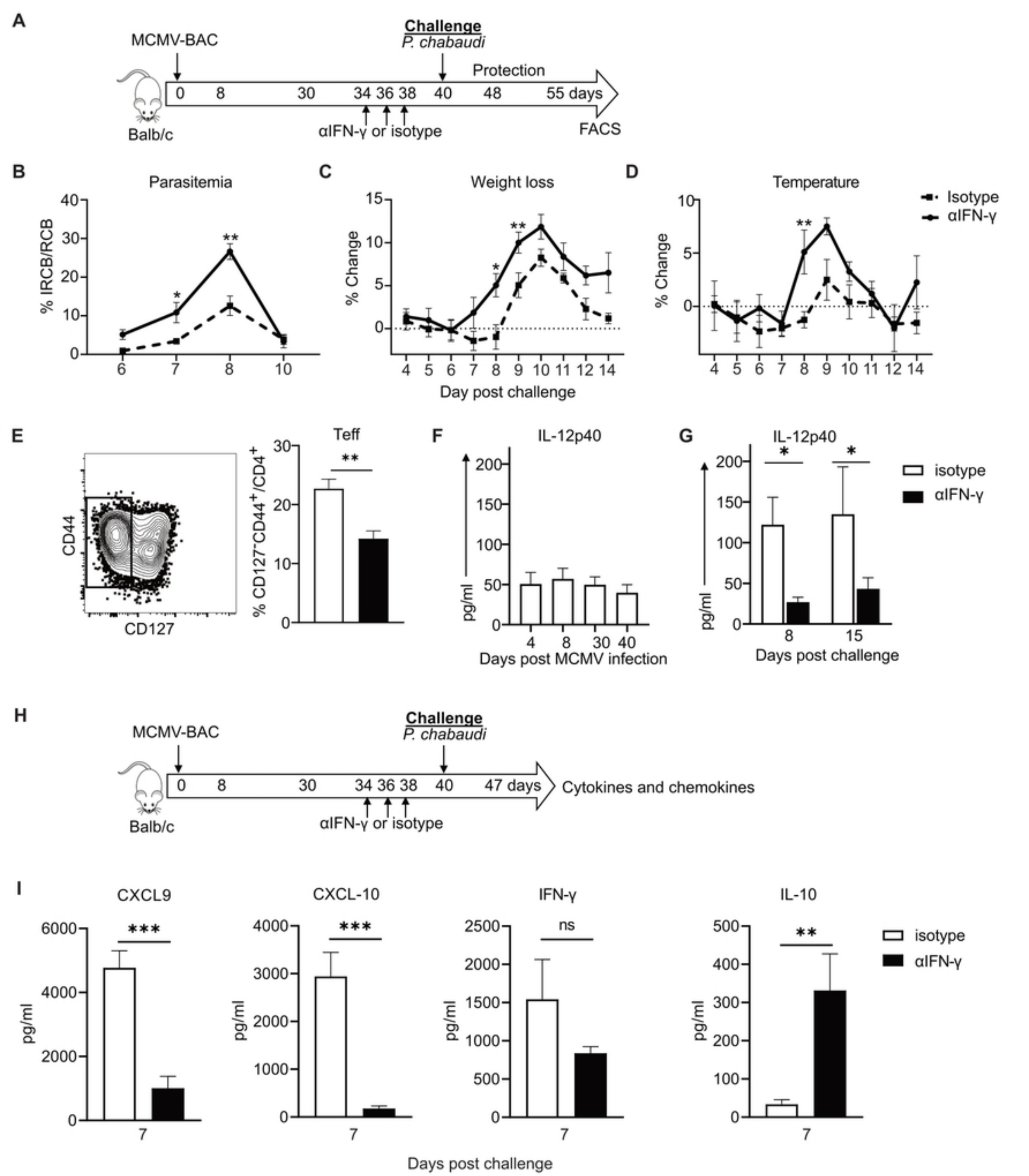
A
MCMV-BAC
Challenge
P. chabaudi
Protection
0 8 30 34 36 38 40 48 55 days
Balb/c
αIFN-γ or isotype
FACS
B
Parasitemia
% IRCB/RCB
C
Weight loss
% Change
Day post challenge
D
Temperature
% Change
Isotype
αIFN-γ
E
CD44
CD127
Teff
% CD127⁻CD44⁺/CD4⁺
F
IL-12p40
pg/ml
Days post MCMV infection
G
IL-12p40
pg/ml
Days post challenge
isotype
αIFN-γ
H
MCMV-BAC
Challenge
P. chabaudi
0 8 30 34 36 38 40 47 days
Cytokines and chemokines
Balb/c
αIFN-γ or isotype
I
CXCL9
CXCL-10
IFN-γ
IL-10
pg/ml
ns
isotype
αIFN-γ
Days post challenge

Figure 5

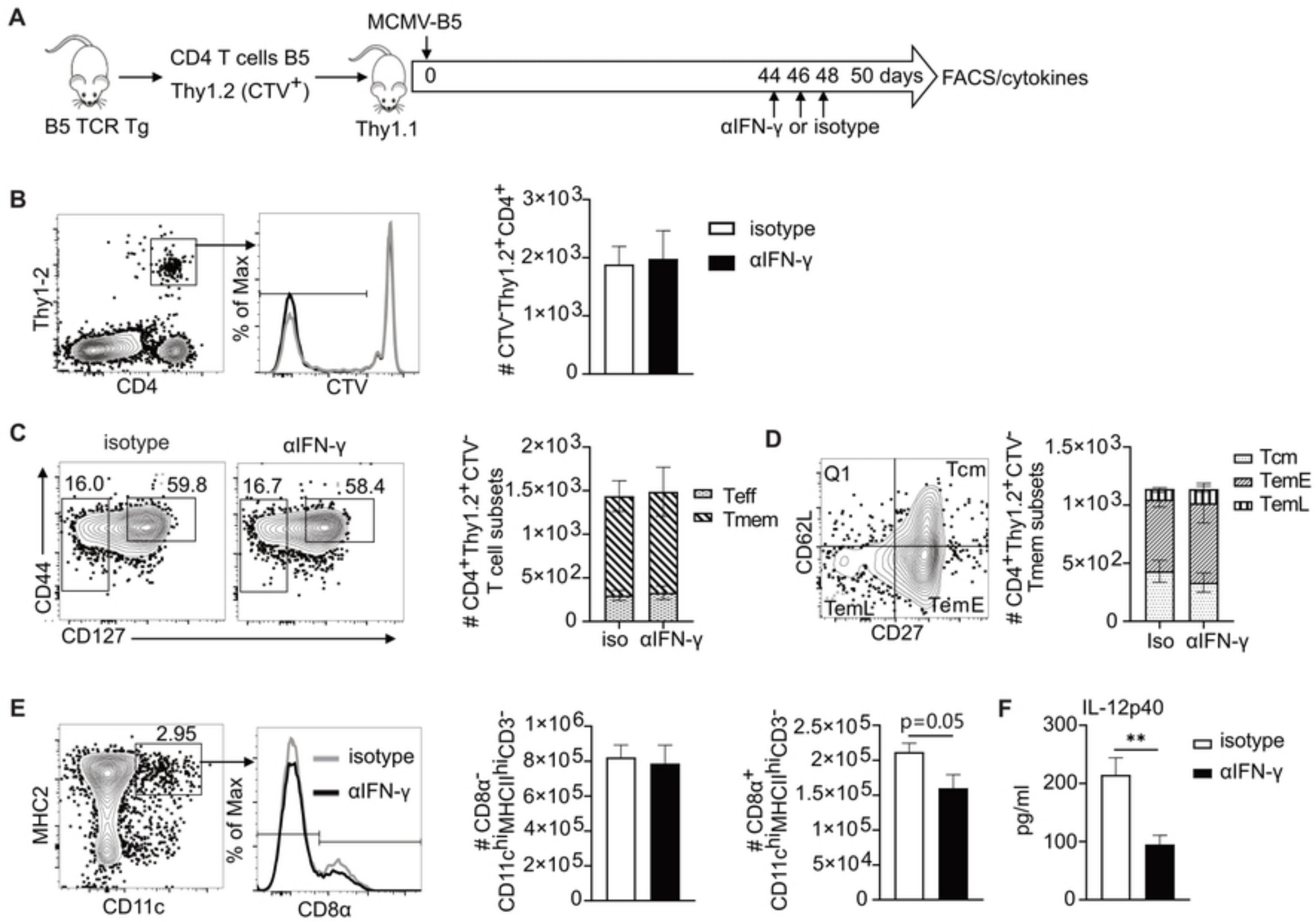
A
MCMV-B5
CD4 T cells B5
Thy1.2 (CTV+)
B5 TCR Tg
Thy1.1
0
44 46 48 50 days
FACS/cytokines
αIFN-γ or isotype
B
Thy1-2
CD4
% of Max
CTV
CTV-Thy1.2+CD4+
isotype
αIFN-γ
C
isotype
αIFN-γ
16.0
59.8
16.7
58.4
CD44
CD127
CD4+Thy1.2+CTV- T cell subsets
Teff
Tmem
iso
αIFN-γ
D
Q1
Tcm
TemL
TemE
CD62L
CD27
CD4+Thy1.2+CTV- Tmem subsets
Tcm
TemE
TemL
Iso
αIFN-γ
E
2.95
MHC2
CD11c
% of Max
isotype
αIFN-γ
CD8α
# CD8α- CD11chiMHCIIhiCD3-
# CD8α+ CD11chiMHCIIhiCD3-
p=0.05
F
IL-12p40
**
pg/ml
isotype
αIFN-γ

Figure 6

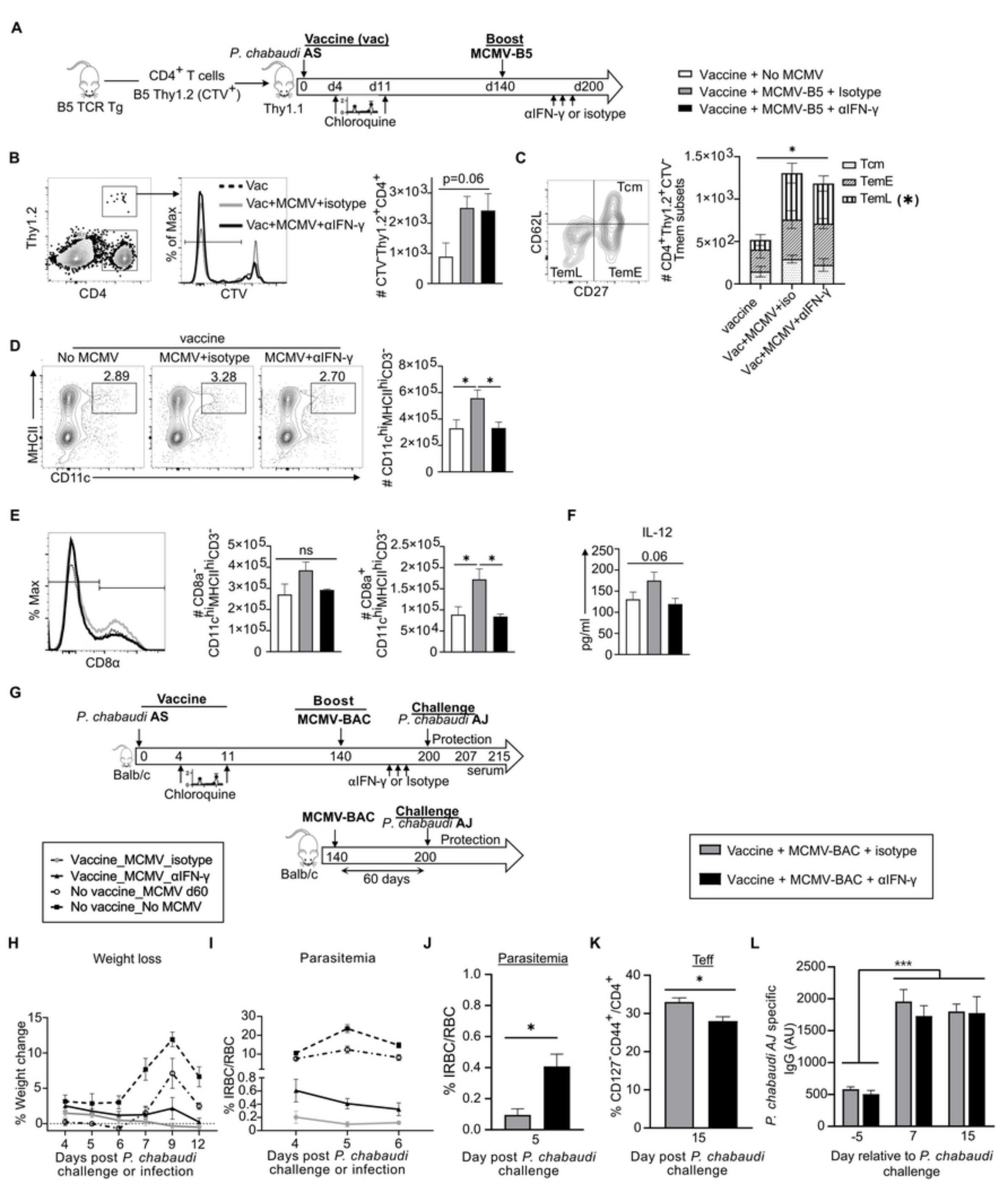
A
Vaccine (vac)
P. chabaudi AS
Boost
MCMV-B5
CD4+ T cells
B5 Thy1.2 (CTV+)
B5 TCR Tg
Thy1.1
0 d4 d11 d140 d200
Chloroquine
αIFN-γ or isotype
Vaccine + No MCMV
Vaccine + MCMV-B5 + Isotype
Vaccine + MCMV-B5 + αIFN-γ
B
Thy1.2
CD4
% of Max
CTV
Vac
Vac+MCMV+isotype
Vac+MCMV+αIFN-γ
p=0.06
# CTV-Thy1.2+CD4+
C
CD62L
CD27
Tcm
TemL
TemE
CD4+Thy1.2+CTV- Tmem subsets
Tcm
TemE
TemL (*)
vaccine
Vac+MCMV+iso
Vac+MCMV+αIFN-γ
D
vaccine
No MCMV
MCMV+isotype
MCMV+αIFN-γ
2.89
3.28
2.70
MHCII
CD11c
CD11chiMHCIIhiCD3-
E
% Max
CD8α
CD8a- CD11chiMHCIIhiCD3-
ns
CD8a+ CD11chiMHCIIhiCD3-
F
IL-12
0.06
pg/ml
G
Vaccine
P. chabaudi AS
Boost
MCMV-BAC
Challenge
P. chabaudi AJ
Protection
0 4 11 140 200 207 215
serum
Balb/c
Chloroquine
αIFN-γ or Isotype
MCMV-BAC
Challenge
P. chabaudi AJ
Protection
140 200
Balb/c
60 days
Vaccine_MCMV_isotype
Vaccine_MCMV_αIFN-γ
No vaccine_MCMV d60
No vaccine_No MCMV
Vaccine + MCMV-BAC + isotype
Vaccine + MCMV-BAC + αIFN-γ
H
Weight loss
% Weight change
Days post P. chabaudi challenge or infection
I
Parasitemia
% IRBC/RBC
Days post P. chabaudi challenge or infection
J
Parasitemia
% IRBC/RBC
Day post P. chabaudi challenge
K
Teff
% CD127-CD44+/CD4+
Day post P. chabaudi challenge
L
P. chabaudi AJ specific IgG (AU)
Day relative to P. chabaudi challenge

Figure 7

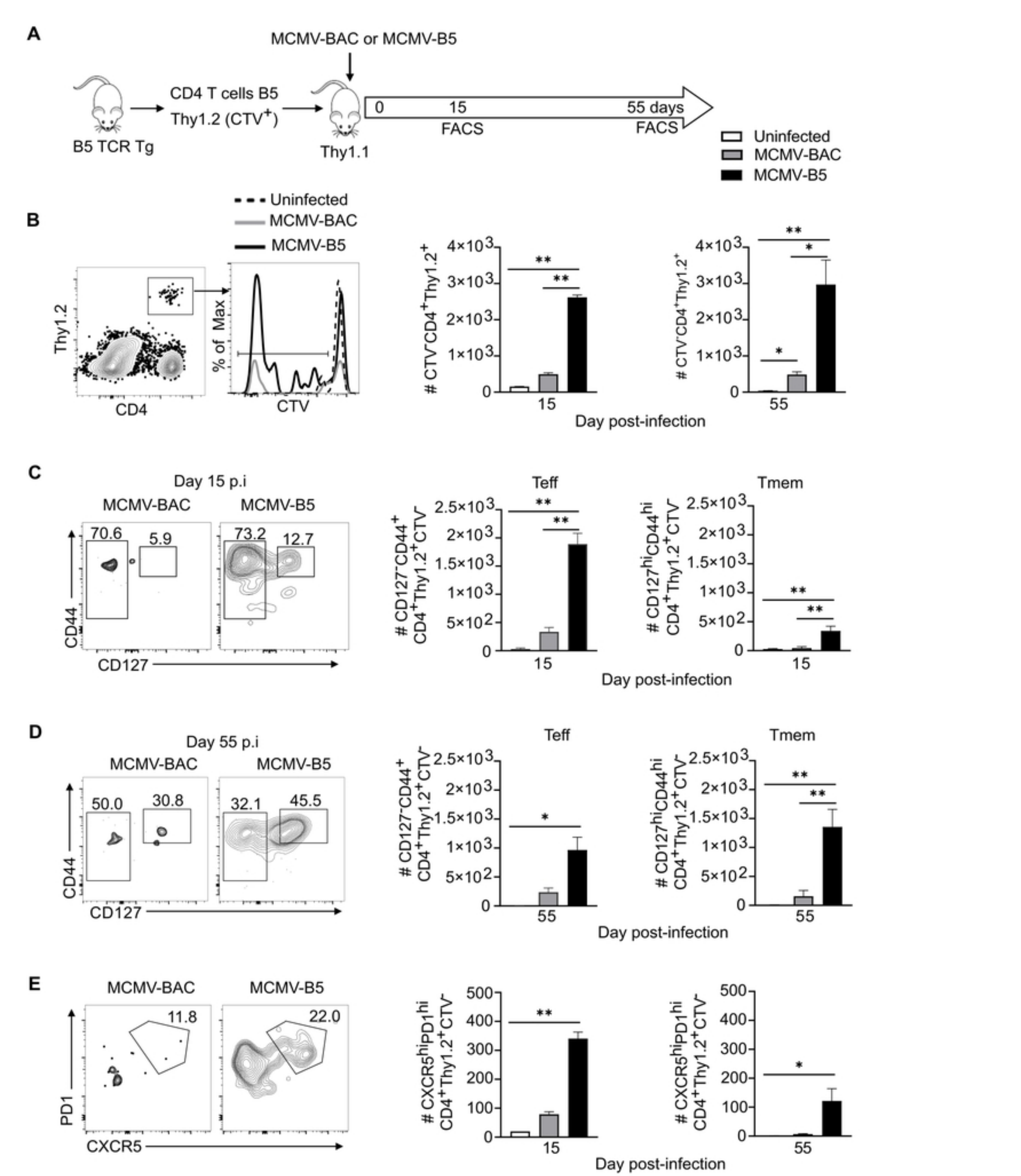
A
MCMV-BAC or MCMV-B5
B5 TCR Tg
CD4 T cells B5
Thy1.2 (CTV+)
Thy1.1
0
15
55 days
FACS
FACS
Uninfected
MCMV-BAC
MCMV-B5
B
Uninfected
MCMV-BAC
MCMV-B5
Thy1.2
CD4
% of Max
CTV
CTV-CD4+Thy1.2+
Day post-infection
C
Day 15 p.i
MCMV-BAC
MCMV-B5
70.6
5.9
73.2
12.7
CD44
CD127
Teff
Tmem
CD127-CD44+ CD4+Thy1.2+CTV-
CD127hiCD44hi CD4+Thy1.2+CTV-
Day post-infection
D
Day 55 p.i
MCMV-BAC
MCMV-B5
50.0
30.8
32.1
45.5
CD44
CD127
Teff
Tmem
Day post-infection
E
MCMV-BAC
MCMV-B5
11.8
22.0
PD1
CXCR5
CXCR5hiPD1hi CD4+Thy1.2+CTV-
Day post-infection

Figure 2